Chapter 10

KINEMATICS AND MASS DISTRIBUTIONS IN SPIRAL GALAXIES

10.1 Introduction

In this set of lectures I will address the questions of the kinematics in spiral galaxies. I will spend some time describing the observational techniques to obtain velocity fields and velocity dispersions and then review the results. This will lead to a discussion of the local and global stability and the mass distributions in spiral galaxies and a comparison to our Galaxy. However, before doing all this I will first give a historical introduction to kinematic observations. Again I will use below distances based on a Hubble constant of 75 km s^{-1} Mpc^{-1}.

The rotation of spiral nebulae was recognized first by Wolf (1914) in M81 and Slipher (1914) in M104 from the inclination of the stellar absorption lines on spectra of the central regions, although the identification of these nebulae as disk galaxies was at that time controversial. That the discovery was made first with absorption lines instead of the more readily observable emission lines can be attributed to observational selection: the central regions of the nebulae were brightest, and the presence there of absorption lines, resembling that of an F- or solar-type star, had been known for a long time. The first observations to result in a plot of the radial velocity versus radius were made by Pease (1916, 1918) for M31 and M104. It was a tedious business, requiring exposure times of about 80 hours for each absorption line spectrum, but the results on M104 showed that the radial velocities relative to the center increased linearly with radius, reaching more than 300 km s^{-1} at a distance of 2.5 arcmin. Pease's measurements along the minor axis

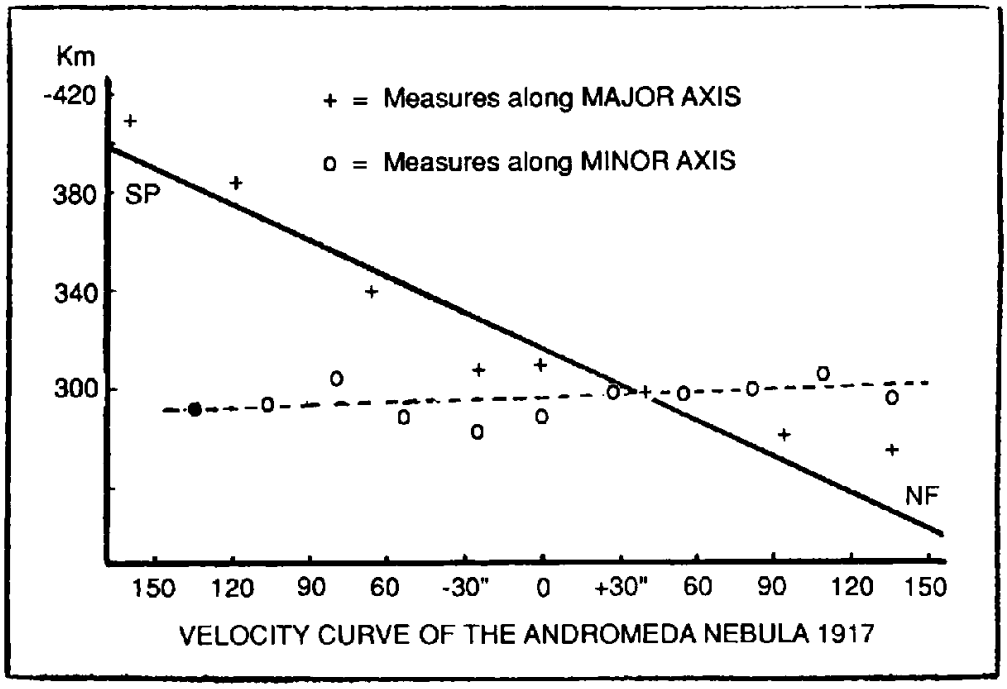

Figure 10.1: Observed velocities in the central part of M31 from absorption line spectra obtained along the major (79 hours) and minor (84 hours) axes with the Mount Wilson 60–inch telescope. These observations provided the first evidence for the rotation of spiral galaxies. From Pease (1918).

of M31 indicated that the radial velocity was nearly constant at all positions, showing that the variation observed along the major axis "is without doubt to be attributed to the rotation of the nebula". The results on M31 are reproduced here in fig. 10.1.

Emission lines from HII regions in the spiral nebulae were discovered about the same time as nebular rotation. Pease (1915) recorded [OIII], Hβ and Hγ in a 34.5 hour exposure of NGC 604 in M33. For galaxies of large angular size, the use of emission lines to study the rotation is hampered by the fact that a single exposure gives only a single point on the rotation curve as a result of the discrete nature of the HII regions. In his classical study of the rotation of M31, Babcock (1939) determined 44 velocity measurements in the inner regions from 236 hours of exposure on the absorption lines, while an additional 56 hours of exposure on emission lines was required to provide 4 more points. These 4 points were, however, very important, for they permitted extension of the rotation curve by a factor of 3 further out into the main part of the disk.

The first detailed observations of the HI at 21 cm wavelength in M31 were made by van de Hulst et al. (1957) using the 25–m Dwingeloo radio telescope with an angular resolution

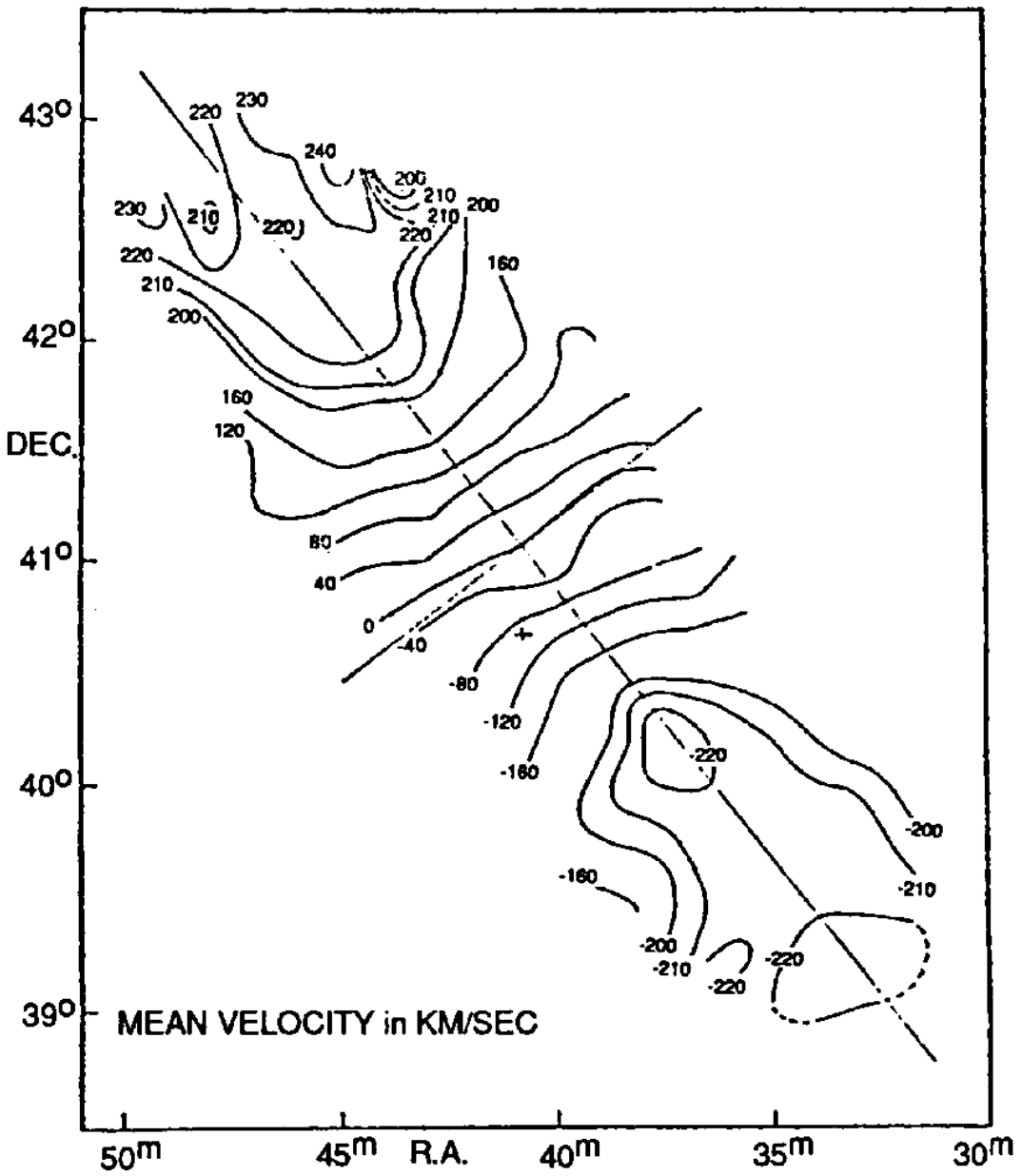

Figure 10.2: The first "spider diagram" to illustrate the observed radial velocity field over the image of a galaxy (here for HI in M31). Velocities are with respect to the systemic velocity and have been multiplied by 1.03 to correct for the inclination. The last is not the usual practice anymore. From Argyle (1965).

of 0.6 degrees. The measurements resulted in a rotation curve from 0.6 to 2.5 degrees from the center, a significant extension of the 1.5 degree last point on Babcock's curve. With a similar angular resolution but improved receiving equipment, Argyle (1965) measured HI profiles over the whole image of M31 and was the first to plot a complete radial velocity field for any galaxy (see fig. 10.2. The resulting "spider diagram" is now in common use. It connects positions of equal radial velocity and gives a good overview of the rotation pattern and possible deviations from circular motion. From it various parameters, such as systemic velocity, position angle of the (kinematical) major axis, inclination and the position of the rotation center can be derived from it in addition to the rotation curve. This will be discussed in more detail below.

10.2 Observational methods for stellar kinematics

The determination of the stellar kinematics in an external galaxy is done from absorption line spectra, where the position and width of a line or a set of lines is compared to that of a Galactic star of the approximate type and luminosity class that dominates the integrated galactic light and therefore the spectrum. Such stars are late G- or early K-giants. The technique used to find the radial velocity and velocity dispersion is nowadays exclusively by Fourier methods (following the fundamental discussion of Simkin, 1971). The basic point is that the galaxy spectrum is the convolution of that of the Galactic giant ("template") and a (often assumed Gaussian) velocity distribution function (also called broadening function). The procedure then is to express the observed galaxy and template spectra as a function of $\log \lambda$, so that velocities and Doppler shifts correspond to linear displacements, and to divide out low-order polynomial fits in order to suppress power at low Fourier frequencies. From there on there are in general three different methods, which will be discussed in turn.

The first (Illingworth and Freeman, 1974) makes use of the peak in the cross-correlation function of the galaxy and template spectra to determine the radial velocity and the slope of the power spectrum to determine the velocity dispersion (larger dispersions result in steeper slopes). With discrete Fourier techniques one calculates the Fourier transforms of the galaxy and template spectra and from this the cross-correlation function between the two and the individual power spectra. The power spectrum of the template is also calculated after its observed spectrum has been broadened by a set of velocity dispersions and the best fitting one is then selected. The template data are in practice noise-free (taken from bright stars), but the galaxy data are not and at high frequencies the galaxy's power spectrum is dominated by the noise in the observations. In most practical cases this noise power spectrum is flat and it can therefore be found over which frequency range in the power spectra the comparison galaxy to template needs to be done. A useful way

of estimating the noise power spectrum is to subtract two observations of the same object (or sky) from one another and use this as the typical noise distribution. A disadvantage of this power spectrum scheme is that the comparison of two power spectra is not easily made objective or automatic and errors have to be estimated also by eye.

The second method is related and makes an exclusive use of the cross-correlation function (Tonry and Davis, 1979), where position and width of its peak are used for radial velocity and dispersion. In that case the width is compared to that of the cross-correlation function of preferably two different templates or otherwise two different observations of the same template star. This method works very efficiently in an automatic way and a routine to estimate formal errors can be incorporated easily. Bottema (1988) has discussed this in detail and has concluded that it is to be preferred in galactic disks where the surface brightness is faint and the dispersions are low. For the practicle case of a disk one has to model the effects of integration along the line of sight on the shape of the broadening function, which in general may result in non-Gaussian functions. The template spectrum can then be convolved with the model function and the resulting cross-correlation peaks can be fitted by a least-squares minimization technique to obtain a best value for the dispersion. The procedure has been illustrated in fig. 10.3.

The third method, which is in widespread use in particular for bright centers of elliptical galaxies and spiral bulges, is the Fourier Quotient method, first introduced by Schechter (see Sargent et al., 1977). This assumes a Gaussian broadening function and makes use of the fact that the Fourier transform of the broadening function is equal to the quotient of the Fourier transforms of the galaxy and template spectra. This quotient is then calculated from the observations and fitted to the Fourier transform of a Gaussian, which is also a Gaussian (but now complex). The problem is, of course that division of noisy data is risky (but there are ways of finding in an objective way which wavenumbers to restrict oneself to) and this method therefore does not work very well for disks.

I will first say a few words about stellar velocity dispersions in spiral bulges before I turn to stellar disks in the next section. There are two aspects. The first is the $V_{\rm m}/\sigma$ versus ε diagram, which measures the importance of rotation relative to the flattening. This diagram has been used extensively to study general aspects of the dynamics of elliptical galaxies and shows that in these systems rotation is not dynamically important enough to provide oblate flattening and that ellipticals are probably triaxial. The most extensive diagram with observed values is the one by Kormendy and Illingworth (1982), which shows that, contrary to ellipticals, bulges generally do follow the oblate, isotropic line. This means that a typical spiral bulge is probably flattened by its rotation (as well as possibly by the disk potential) and that the velocity distribution is more or less isotropic (at least in the central parts). This general relation can be used with values for the bulge of the Galaxy to estimate its flattening and in my first set of lectures above I derived an axis ratio of 0.7 ± 0.15.

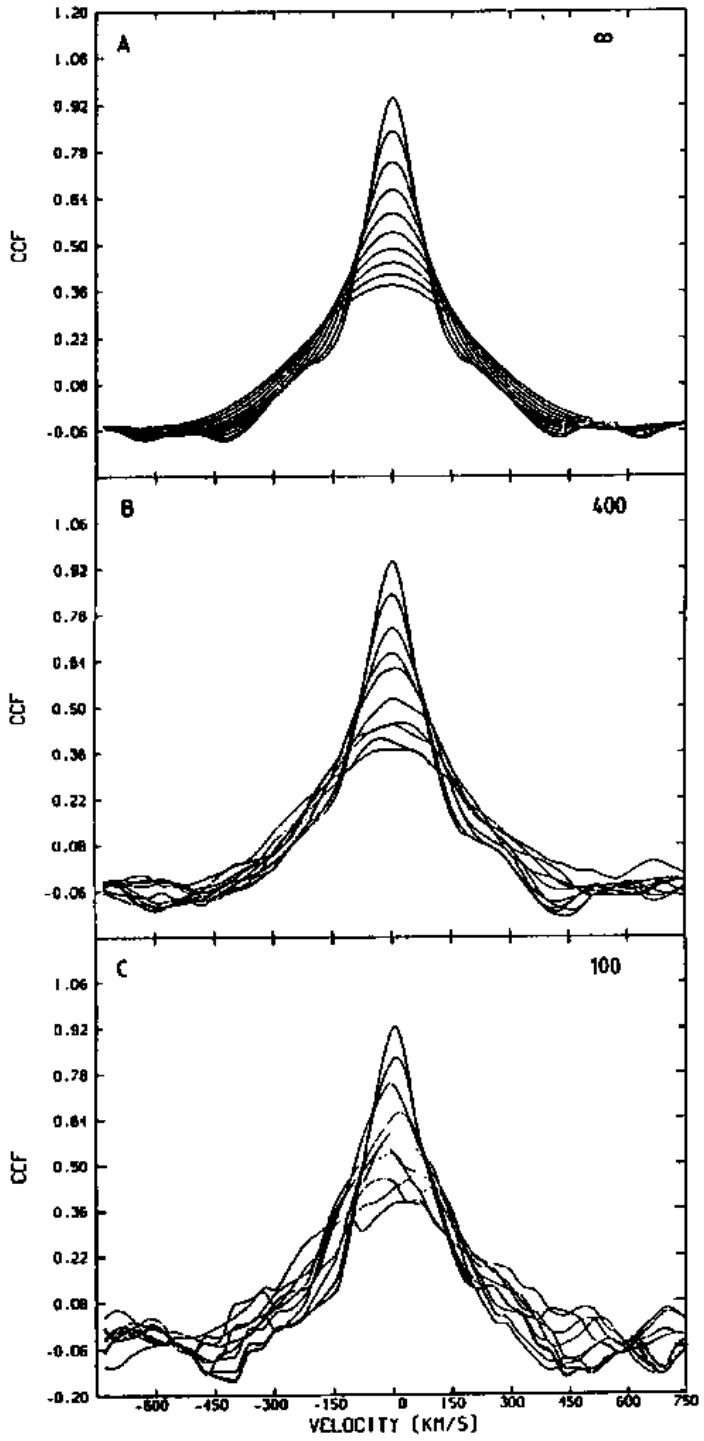
A
∞
B
400
C
100
CCF
VELOCITY (KM/S)

Figure 10.3: Cross-correlation peaks between the spectrum of a K0III star with the same spectrum after convolution with Gaussian broadening functions with dispersions from 18.2 to 182 km s^{-1} and addition of artificial noise. At the top there is no noise, in the middle panel the noise is that expected for a count level of on average 400 in each of the 600 spectral elements, while in the lower it is 100. Note that the peaks have the same maximum at each dispersion independent of the count level, but that they become more irregular for noisier data. From Bottema (1988).

The second relation is that between the velocity dispersion and the bulge luminosity (Kormendy and Illingworth, 1983). This relation is interesting, because it can be used to derive information on how prominent the bulge of our Galaxy would appear from an external viewpoint. As before I use a velocity dispersion of 110±10 km s^{-1}. Then it follows that M31 (150–160 km s^{-1}) and M81 (160–170 km s^{-1}) have bulges that are at least 5 and at most 10 times more luminous than the bulge of the Galaxy. On the other hand at least the disk of M31 has a radial scalelength that is very similar to that of the disk of the Galaxy, so that these bulges are also brighter relative to the disk than is the case in the Galaxy. This is important to realize, because in the semi-popular literature and in elementary textbooks one often sees one of these two galaxies illustrated as examples of what the Galaxy would look like as seen from outside. I will return to this point later in this course, when I discuss the possible Hubble type of the Galaxy.

The data given above using the $V_{\rm m}/\sigma - \varepsilon$ relation seem to suggest that the velocity distribution in the central parts of bulges is not too far from isotropic. This can be checked for the case of the early type spiral NGC 7814, where a formal estimate of the velocity anisotropy can be made (van der Kruit and Searle, 1982b). This galaxy has a luminosity distribution that is dominated by the bulge (it contains 93% of the light), but it still contains HI in the disk, so that the circular velocity can be measured and combined with stellar rotation and velocity dispersion in the bulge. This is a unique situation that usually does not occur in ellipticals (when HI is seen, it is unclear whether it is in circular rotation), S0 galaxies (where HI is observed at larger radii than where the stellar kinematics can be measured) or later type spirals (where the disk potential is a major contributor).

If we assume that one of the principal axes of the velocity ellipsoid is perpendicular to the plane and the stellar space density goes as $R^{-\beta}$, it follows that in the plane we have

$$V_{\rm rot}^2 = V_{\rm t}^2 - R\frac{\partial\langle V_{\rm R}^2\rangle}{\partial R} + (\beta-1)\langle V_{\rm R}^2\rangle + \langle (V_\theta - V_{\rm t})^2\rangle. \qquad (10.1)$$

$V_{\rm rot}$ is the circular velocity related to the radial force $-K_{\rm R} = V_{\rm rot}^2/R$, $V_{\rm t}$ the rotation velocity of the bulge stars and $\langle V_{\rm R}^2\rangle$ and $\langle (V_\theta - V_{\rm t})^2\rangle$ the squares of the radial and tangential velocity dispersions. From HI kinematics, optical surface photometry and stellar

kinematics along a line just above the dust lane we know all parameters, except the radial velocity dispersion (the tangential one is in the line of sight). It is observed that in the bulge between 40 and 90 arcsec (2.9 to 6.5 kpc) $V_{\rm rot}$, $V_{\rm t}$ and the tangential velocity dispersion are all constant with R, and it then follows that we must have

$$\langle V_{\rm R}^2 \rangle = \frac{V_{\rm rot}^2 - V_{\rm t}^2 - \langle (V_\theta - V_{\rm t})^2 \rangle}{\beta - 1} + \alpha R^{(\beta-1)}. \tag{10.2}$$

Here, α is an integration constant. From the observed velocity dispersion on the minor axis and the numerical values of the other parameters it follows for NGC 7814 that α must be positive and that therefore the radial velocity dispersion increases with radius. In the inner regions the velocities are indeed roughly isotropic, but become increasingly anisotropic with the radial dispersion exceeding the tangential one. In the Galaxy Woolley (1978) finds that the velocity ellipsoid of field RR Lyrae stars in the solar neighborhood belonging to the halo population is also highly anisotropic with the radial dispersion exceeding the tangential one.

10.3 Observations of stellar kinematics in disks

The measurement of the stellar velocity dispersions of the old disk populations serves a number of purposes. The first is the possibility to estimate the disk mass distribution independently from the rotation curve (see below), which provides useful constraints on the mass distribution in the dark halo. In the second place, the velocity dispersion plays a role in both the global and the local stability of galaxy disks. Gravitational instability has been a major subject of theoretical study ever since it was described originally by Newton in his famous laws. It actually was Newton himself, who worried in his correspondence with Dr. Bentley about what kept the sun and the fixed stars from collapsing together in a static universe. He proposed that stars were distributed evenly in space and that therefore all gravitational pulls would compensate each other. From the distribution of stars on the sky as a function of apparent magnitude (taken to indicate distance) he inferred that at least for the brightest stars (to fourth magnitude) their numbers occurred in the required ratio's to conform to spacial uniformity and homogeneity. But such a distribution is of course very difficult to bring about and even if this were possible at all, the supposed equilibrium was necessarily very unstable. The solution is of course that the equilibrium is maintained by the relative random motions of the stars. The problem was early this century reformulated by Jeans in the form of the now-called "Jeans instability criterion" in an infinite, homogeneous medium. His criterion states that for a given mass density and temperature (or velocity dispersion) masses above a certain critical mass are unstable to their own gravity and will collapse. The larger the velocity dispersion and the smaller the density is, the larger this critical mass becomes ($M_{\rm Jeans} \propto \langle V^2 \rangle^{3/2} \rho^{-1/2}$).

It is therefore also not at all obvious why stellar disks are smooth and stable. Of course, in particular the younger populations display spiral structure, which will be some kind of instability, but not of a violent type that completely redistributes the matter in the disk. On the other hand, the old disk population is generally speaking smooth, as is clearly seen in the disks of S0 galaxies, where young populations are absent. It is known that rotation in galactic disks can only stabilize low-wavenumber modes and that the finite thickness of disks may be relevant at small wavelengths (Goldreich and Lynden-Bell, 1965). The local stability of thin stellar disks was addressed by Toomre (1964), who showed that the stellar velocity dispersion needs to exceed a certain critical value to ensure stability against local axisymmetric modes. It is usually translated in the parameter Q, which has to exceed unity for local stability. This parameter is given by

$$Q = \frac{\langle V_{\rm R}^2 \rangle^{1/2} \kappa}{3.36 G \sigma}, \tag{10.3}$$

where κ is the epicyclic frequency $\kappa = 2\{B(B-A)\}^{1/2}$ with A and B the local Oort constants and σ the disk surface density. This criterion is the equivalent of the Jeans instability in an infinite, homogeneous medium, reformulated for a flat stellar disk. Global (bar-like) modes can be suppressed by a hot component (of high velocity dispersion), which may either be a dark halo such as the ones that may produce the observed flat rotation curves (Ostriker and Peebles, 1973) or the old disk population itself, if it has a high velocity dispersion in its inner regions (Sellwood, 1983; Athanassoula and Sellwood, 1986). The dispersion of the old disk population required corresponds to values of Q of the order of 2.

It has been known for a long time that the stellar velocity dispersion in disks is a result of secular evolution of the kinematics of the stars. This is evident for example from the observed relation between the age of the stars and their velocity dispersion in the solar neighborhood in the Galaxy (e.g. Wielen, 1977). Spitzer and Schwarzschild (1951) were the first to propose a mechanism for this effect, namely scattering of the stellar orbits by massive gas concentrations in the interstellar medium. Such concentrations are now known to exist in the form of giant molecular clouds, but it is at present unclear whether these occur in sufficient numbers to provide the observed change of kinematics for the solar neighborhood or whether this process may give the actual axis ratio's of the local velocity ellipsoid (e.g. Lacey, 1984). It may very well be that spiral structure (either in the form of density waves or transient mass density disturbances) also is important in this respect, but I will not discuss this here in detail.

We have seen that edge-on disks show that the vertical scale parameter of the old disk population is independent of galactocentric distance. For the isothermal sheet approximation the relation between the scaleheight $z_{\rm o}$ in the density distribution $\mathrm{sech}^2(z/z_{\rm o})$, the

surface density $\sigma(R)$ and the velocity dispersion is

$$\langle V_z^2 \rangle_* = \pi G \sigma(R) z_o. \tag{10.4}$$

If z_o is not a function of R and if $\sigma(R)$ is an exponential with scalelength h, then it follows that

$$\langle V_z^2 \rangle_*^{1/2} = \{\pi G \sigma(0) z_o\}^{1/2} \exp(-R/2h). \tag{10.5}$$

So, if the old disk populations have an M/L ratio independent of galactocentric distance, we expect that the vertical velocity dispersion drops with R as an exponential with an e-folding of twice the scalelength of the surface brightness distribution. This is open to observational confirmation. The first detailed check of this prediction was made by van der Kruit and Freeman (1986) on the face-on spiral NGC 5247. The data are illustrated in fig. 10.4 and reach out to about 2 optical scalelengths. This is not very far out into the disk, but this work already required a total exposure of 8.8 hours with the 3.9 m Anglo-Australian Telescope, which indicates the difficulty of obtaining such observations as a result of the low surface brightness and small dispersions. The least-squares fit, indicated by the dashed line, has an e-folding of 2.4±0.6 optical scalelengths and is in good agreement with the predictions and therefore with no change in M/L with radius. Note that the central z-velocity dispersion is about 60 km s^{-1} and certainly not dynamically insignificant. Bottema (1988 and work in progress) has confirmed this conclusion for a few more spirals. More evidence that M/L for the old disk population is constant with radius will be discussed below, but in what follows I will always make this assumption. From edge-on galaxies we know mean values for the vertical scale parameter zo and from this we can estimate values for the surface density and M/L from the vertical velocity dispersion (and the surface brightness). The latter comes out around 6 in solar B-units for the old disk population exclusively.

The constant vertical scaleheight of the old disk population as a function of radius provides us with a prediction for the radial dependence of the vertical velocity dispersion. No such a priori prediction exists for the dispersions parallel to the plane, although we know from fundamental galactic dynamics that the ratio of the radial and tangential dispersions is related to the local Oort constants as

$$\frac{\langle (V_\theta - V_t)^2 \rangle}{\langle V_R^2 \rangle} = \frac{B}{B - A}. \tag{10.6}$$

There is however already evidence that these velocity dispersions must decrease with galactocentric distance from the observation of the sharp edges to the radial light distribution. At these radii the exponential decline is 1 kpc or less. At a typical radius of 20–25 kpc and a rotation curve of 200–250 km s^{-1} the stars will go through epicycles with half-axes in the R-direction of about 1 kpc, if their random motions are 10–15 km s^{-1}.

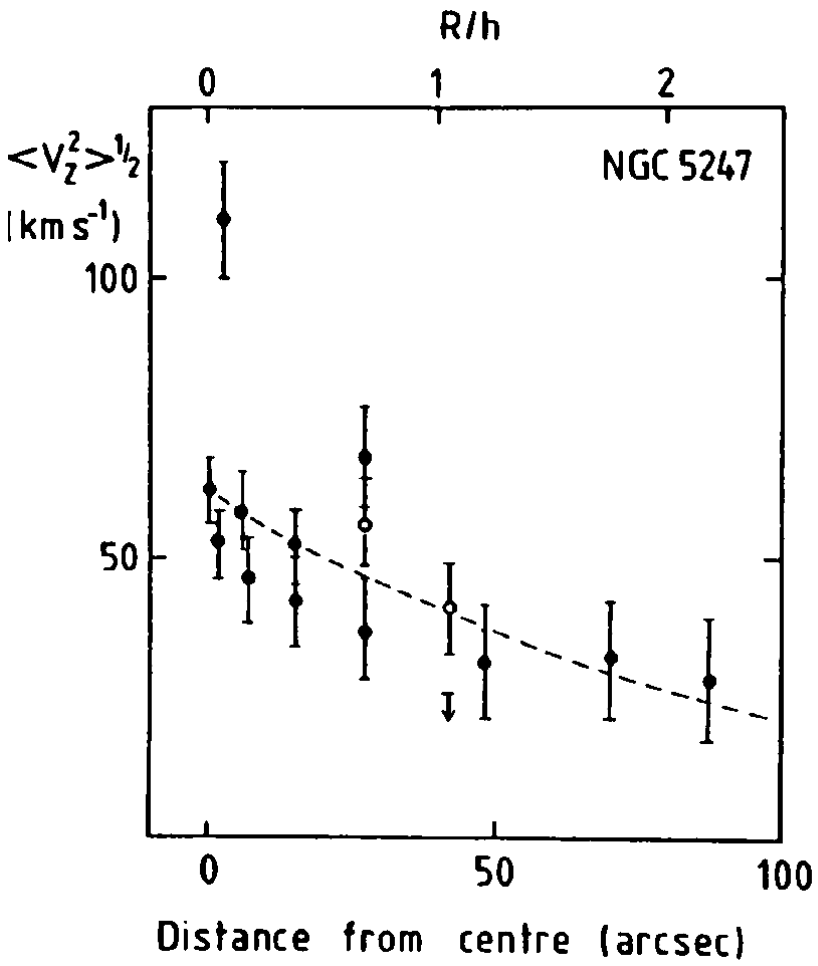

Figure 10.4: The observed velocity dispersion of the old disk population in the face-on spiral NGC 5247. The galactocentric distance R has been expressed at the top in units of the optical scalelength h of the disk. The dashed line is a least-squares fit to the points and is consistent with a decline with an e-folding of $2h$. From van der Kruit and Freeman (1986).

This is much lower than e.g. in the solar neighborhood, so that we may indeed expect these velocity dispersions to drop as well with increasing radius. It can also be shown for the Galactic disk, that unless $\langle V_{\rm R}^2 \rangle^{1/2}$ decreases with radius, Toomre's stability parameter Q will become less than unity a frew kpc inward from the solar position.

There are two independent ways in which observations can reveal values for parallel velocity dispersions. The first is by direct measurement in highly inclined galaxies, but

then one has to make corrections for the integration along the line of sight. Such corrections are in practice straightforward to make. The second method is by measuring the asymmetric drift. This is the effect that in a disk in equilibrium the mean tangential velocity $V_{\rm t}$ of a mass component is less than the circular velocity (corresponding to a centrifugal force necessary to compensate the gravitational force) by an amount that depends on the velocity dispersion. The random motions provide a pressure support, so that a mean tangential velocity less than the circular velocity is required. The relevant equation is

$$-K_{\rm R} = \frac{V_{\rm t}^2}{R} - \langle V_{\rm R}^2\rangle \left[\frac{\partial}{\partial R}(\ln \nu\langle V_{\rm R}^2\rangle) + \left(\frac{1}{R}\right)\left\{1 - \frac{\langle (V_\theta - V_{\rm t})^2\rangle}{\langle V_{\rm R}^2\rangle}\right\}\right] + \langle V_{\rm R}V_{\rm z}\rangle \frac{\partial}{\partial z}(\ln \nu\langle V_{\rm R}V_{\rm z}\rangle). \tag{10.7}$$

Here ν is the stellar density distribution, $K_{\rm R}$ the radial force and $V_{\rm t}$ the mean stellar tangential velocity. The last term, which contains the cross-term $\langle V_{\rm R}V_{\rm z}\rangle$, is small. In the case that the velocity ellipsoid points toward the galactic center, the term can be shown to reduce to $(1/R)(1 - \langle V_{\rm z}^2\rangle/\langle V_{\rm R}^2\rangle)$ and this is probably the largest value this term may take. There is even a compelling reason to ignore the term altogether, if the galaxy has a flat rotation curve, as was first pointed out by van der Kruit and Freeman (1986). For an axially symmetric system Poisson's equation is

$$\frac{\partial K_{\rm R}}{\partial R} + \frac{K_{\rm R}}{R} + \frac{\partial K_{\rm z}}{\partial z} = -4\pi G\rho. \tag{10.8}$$

Now near the plane the first two terms on the left are equal to $2(A - B)(A + B)$. In area's away from the central regions, where we have flat rotation curves, $A = -B$ and the terms vanish. So, for a flat rotation curve the plane-parallel case (with no cross-terms involving U and W) happens to be an excellent approximation. The stellar dynamics is then independent of the radial gradients, there is no reason for the velocity ellipsoid to point towards the galactic center and we expect it to be parallel to the plane over the range of z occupied by the old disk, at least over the relevant extent in z (most old disk stars are at $z < z_{\rm o}$).

We then may represent the ratio of the two velocity dispersions in terms of the Oort constants as given above and write $-K_{\rm R} = V_{\rm rot}^2/R$. For the exponential disk with constant thickness (and M/L) the density distribution of the old disk population ν gives rise to $\partial(\ln \nu)/\partial R = -1/h$. Then we have

$$V_{\rm rot}^2 - V_{\rm t}^2 = \langle V_{\rm R}^2\rangle \left\{\frac{R}{h} - R\frac{\partial(\ln\langle V_{\rm R}^2\rangle)}{\partial R} - \left[1 - \frac{B}{B - A}\right]\right\}. \tag{10.9}$$

Now we can measure h from surface photometry and $V_{\rm rot}$, A and B for the gas from optical emission lines or 21–cm HI mapping. The latter is so, because the gas has a very

Table 10.1: Q as a function of radius

$R/h = 1.0$	"Q" = 1.17
1.5	1.00
2.0	0.96
3.0	1.06
4.0	1.31
5.0	1.73

low velocity dispersion and therefore for the gaseous component $V_{\rm t}$ is very close to $V_{\rm rot}$. The only unknown in the equation above then is the radial velocity dispersion and its radial derivative.

For illustrative purposes we can calculate the radial dependence of the stellar velocity dispersion for a disk with a flat rotation curve. Then $B/(B-A) = 0.5$. First we may assume that the ratio of vertical to radial velocity dispersion is always the same (although there is no theoretical reason for this); then we have

$$\langle V_{\rm R}^2 \rangle^{1/2} \propto \exp(-R/2h) \tag{10.10}$$

and

$$V_{\rm rot}^2 - V_{\rm t}^2 = \langle V_{\rm R}^2 \rangle (2R/h - 0.5). \tag{10.11}$$

The other possibility would be that the disk will during its evolution heat up to an equilibrium value for Q that is roughly constant with galactocentric distance. E.g. Sellwood and Carlberg (1984) find such a behavior in their numerical experiments at a value of Q around 1.7 or so. This implies for a flat rotation curve (when $\kappa = (2V_{\rm rot}^2/R^2)^{1/2}$) that

$$\langle V_{\rm R}^2 \rangle^{1/2} \propto R \exp(-R/h) \tag{10.12}$$

and

$$V_{\rm rot}^2 - V_{\rm t}^2 = \langle V_{\rm R}^2 \rangle (3R/h - 2.5). \tag{10.13}$$

Over the ranges where the stellar velocity dispersion can be measured the difference is actually small (see also Martinet, 1988). To illustrate this the following table gives Q as a function of radius (arbitrarily normalized to unity at $R = 1.5h$) for the first case.

For $R < h$ the rotation curve is generally not flat and the approximation used must fail. We see that Q only starts to increase significantly beyond $R = 3h$ and there it is impossible to measure stellar kinematics. The conclusion then is that at present we cannot distinguish between the two possibilities from stellar spectroscopy alone. On the other hand at larger R there is a significant contribution from the gas to the disk surface

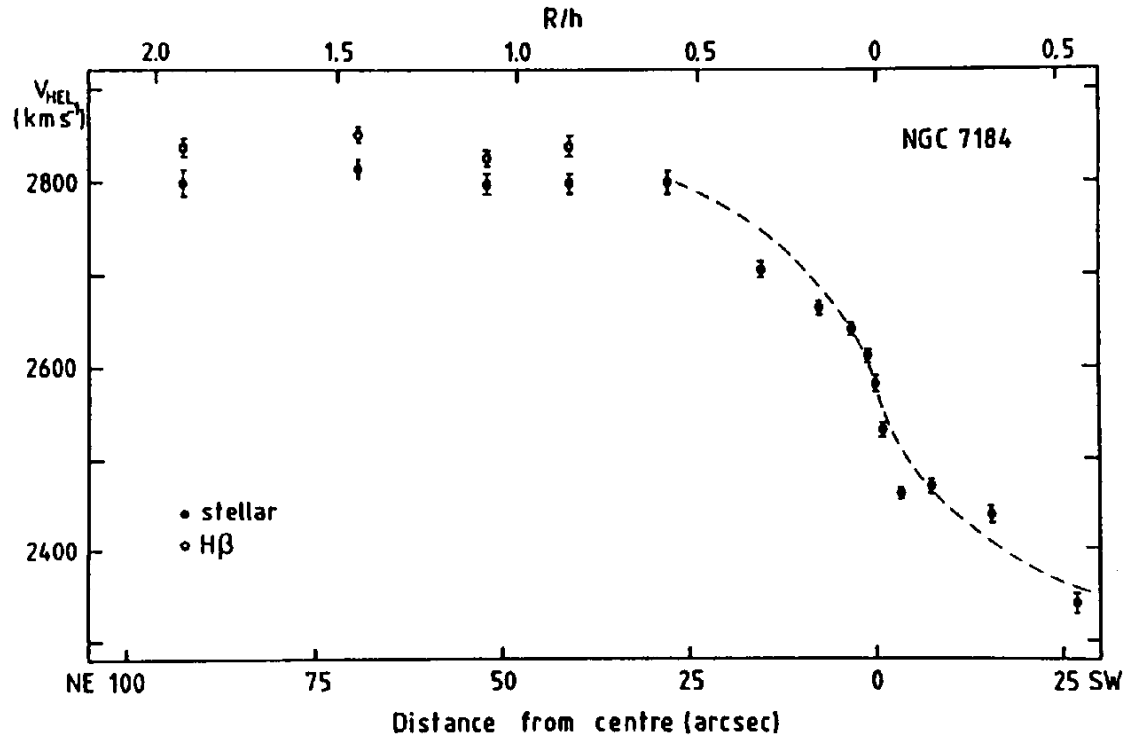

Figure 10.5: The asymmetric drift between the stars and the gas in the disk of NGC 7184 is evident from the displacement of the observed rotation curves for these two components. The data have not been corrected for inclination and derive from the same spectra. The dashed line shows a symmetric stellar rotation curve for the central area's. The top scale gives the radial distance in units of the photometric scalelength h. From van der Kruit and Freeman (1986).

density. The calculation of Q then has to involve a "mean" velocity dispersion between stars and gas and a higher surface density than the exponential stellar disk. This may easily lower the value of "Q" by a factor up to two, so that the increase predicted above can in actual galaxies very well be compensated by the gas. With this in mind we may say that the two assumptions are likely to be very similar in actual galaxies.

The method then is to measure $V_{\rm rot}$ from the gas, $V_{\rm t}$ from the stars and h from surface photometry and then to fit these data to a radial dependence of the radial velocity dispersion. This was first done by van der Kruit and Freeman (1986) for NGC 7184 and over the radial extent R/h between 1 and 2. The observed asymmetric drift between the stars and the gas is illustrated in fig. 10.5. The data are consistent with the models just given and imply a radial velocity dispersion of about 100–120 km s^{-1} at $R/h = 1.0$ (NGC 7184 has a $V_{\rm rot}$ of 266 km s^{-1}) and a value of Q of about 1.5 to 2, if the M/L of the old

disk is 6 in solar B-units. Again Bottema (1988 and in preparation) has confirmed the conclusion of a roughly constant Q (of order 2) out to 2 or 3 scalelengths in other spirals, while Martinet (1988) has argued for this conclusion on general, theoretical grounds.

Before leaving the subject of stellar kinematics, a few words need to be said on the origin of the observed radial variation of the velocity dispersions with galactocentric distance and on variations between galaxies. The equilibrium situation in disks is apparently such that the radial velocity dispersion of the stars is close to that necessary to keep Q constant and ensure marginal local stability, while the vertical one decreases with a radial e-folding of two luminosity (and density) scalelengths in order to keep the old disk thickness constant. I have illustrated above that, when effects of the gas on the value of Q are taken into account, these two properties may in practice arise in the simple case of a constant axis ratio of the velocity ellipsoid. The constant Q may arise from the fact that disks heat until this situation has been established, after which suppression of large instabilities then feeds back into less heating, as is indeed observed in numerical experiments (Sellwood and Carlberg, 1984). Note that the central velocity dispersion is then so large that it also suppresses global stabilities (Sellwood, 1983; Athanassoula and Sellwood, 1986) and this may just as well be part of the feedback cycle.

Bottema (1988) has found that the radial stellar velocity dispersion at one scalelength from the center correlates with the rotation velocity of the flat rotation curve and therefore through the Tully-Fisher relation also with the integrated luminosity. An up-to-date version of his relation is shown in fig. 10.6, where the horizontal axis is the luminosity of the old disk only. Face-on galaxies have been added with the vertical velocity dispersion at the center. For the exponential decline described above the dispersion at $R = h$ will be a factor $e^{-1/2} = 0.61$ lower than at the center, which is about the ratio of vertical to radial velocity dispersion of the stars in the disk of the Galaxy near the sun, so this central value of the vertical dispersion should be comparable to the radial one at one scalelength. The correlation can be understood qualitatively as follows. Assume again a flat rotation curve with rotation velocity $V_{\rm m}$ and an exponential disk with central surface brightness $\mu_{\rm o}$ and constant M/L. The radial velocity dispersion at one scalelength h can then be written as

$$\langle V_{\rm R}^2 \rangle_h^{1/2} \propto \mu_{\rm o}(M/L)Qh/V_{\rm m}. \tag{10.14}$$

Noting that the disk luminosity L is proportional to $\mu_{\rm o}h^2$, we get

$$\langle V_{\rm R}^2 \rangle_h^{1/2} \propto \mu_{\rm o}^{1/2}(M/L)QL^{1/2}/V_{\rm m}. \tag{10.15}$$

Taking the Tully-Fisher relation as $L \propto V_{\rm m}^{\rm n}$ replaces $V_{\rm m}$ by $L^{1/{\rm n}}$. A reasonable value for n is about 4, so that over a range in L of 4 magnitudes the velocity dispersion is predicted to increase by a factor 2.5, similar to what is seen in fig. 10.6, if indeed $\mu_{\rm o}$, M/L and Q are constant from galaxy to galaxy. The constancy of $\mu_{\rm o}$ is "Freeman's law" and has

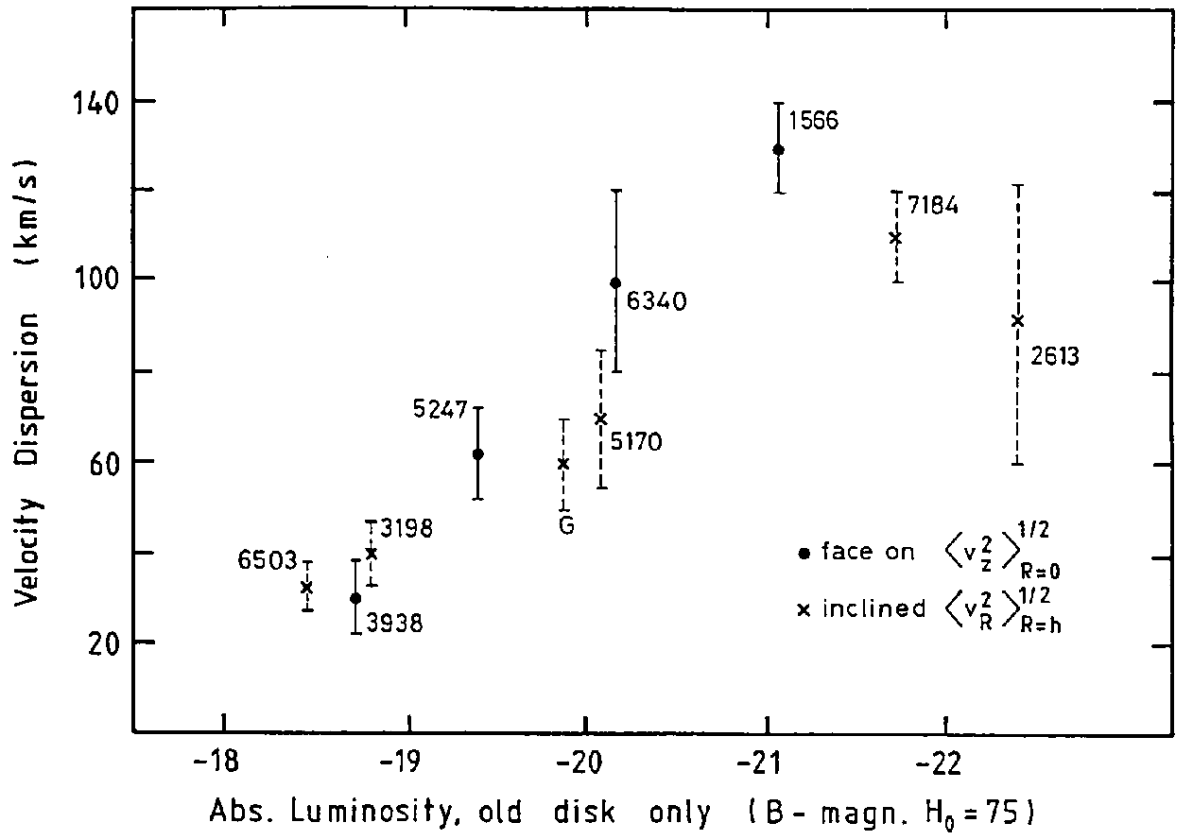

Figure 10.6: The stellar velocity dispersion in galactic disks as a function of the integrated magnitude of the old disk component. For inclined galaxies (crosses) the observed radial velocity dispersion at one photometric scalelength from the center has been plotted; for face-on galaxies (dots) the vertical velocity dispersion at the center is entered. From Bottema (private communication).

been presented already above and its possible origin will be discussed later. It then is a remarkable property of galactic disks, that M/L (resulting from the mass spectrum of stars at birth, the so-called initial mass function) and Q (resulting from dynamical heating) or at least the product of these two, are independent in first approximation of the mass of the galaxy. Note that the Galaxy is also included in the figure, using the data from Lewis (1986, see also Lewis and Freeman, 1989) and that the point fits rather well with the external galaxies.

10.4 Observations of the kinematics and distribution of the gas

The distribution and kinematics of the gas can be observed using optical emission lines, such as Hα, Hβ, [OIII], etc. or radio lines, such as the 21–cm line of HI or molecular lines as from CO. The older method of optical slit spectroscopy will not be discussed here in detail and I will concentrate on observations that map the velocity field over a large part of the galaxy. In principle a large number of slit positions can be used for this also, while in the radio a velocity field can in principle be found from a large number of observations at individual positions with a single-dish instrument. The fastest method these days is the use of interferometric techniques. In the radio this is done with the use of aperture synthesis telescopes, such as at Westerbork or the VLA. At optical wavelengths the last few years have seen the advent of scanning Fabry-Perot instruments, such as TAURUS.

The detailed workings of such instruments will not be discussed here and I will limit myself to saying that one ends up after observation and calibration (both in position, intensity and wavelength) with a set of so-called channel maps. These are maps of the intensity on the sky in a small range of wavelength or radial velocity. A set of maps contiguous in radial velocity make up the "data-cube" (two spacial and one velocity dimension) and it is this information that is used to derive the desired kinematics. One critical procedure that proceeds all analysis is the subtraction of the continuum emission, which is derived by averaging all maps at velocities outside the range present in the galaxy.

There are two methods to derive the maps of parameters, that one wishes to determine, namely integrated intensity, radial velocity and velocity dispersion. These are of course related at each position to the first three moments of the intensity distribution as a function of velocity, the so-called profile. The first method directly determines these moments. However, the velocity ranges outside the line emission from the galaxy contain noise that in particular in area's of low signal-to-noise have devastating effects on the first and second moments, while it is always unwise to add unnecessary noise in the calculation of the zeroth moment. One overcomes this by defining a "window" in velocity at each position, over which emission from the galaxy is observed. This can be done automatically, but it is much better to do this interactively by displaying cuts through the data-cube on a television screen. These cuts have a spacial (e.g. R.A. or Dec) and a velocity dimension and are often referred to as "$l-V$ diagrams". One then uses a cursor to define at each sky position the velocity extent over which galaxy emission is present in this diagram. Only the regions within the window are then used to calculate the moments. This method is in principle sensitive to personal bias and may depend on the (usually color) display levels on the monitor.

The second procedure is to fit a Gaussian to each individual profile and determine the kinematic parameters in this way. The advantage of the window method is that it does not

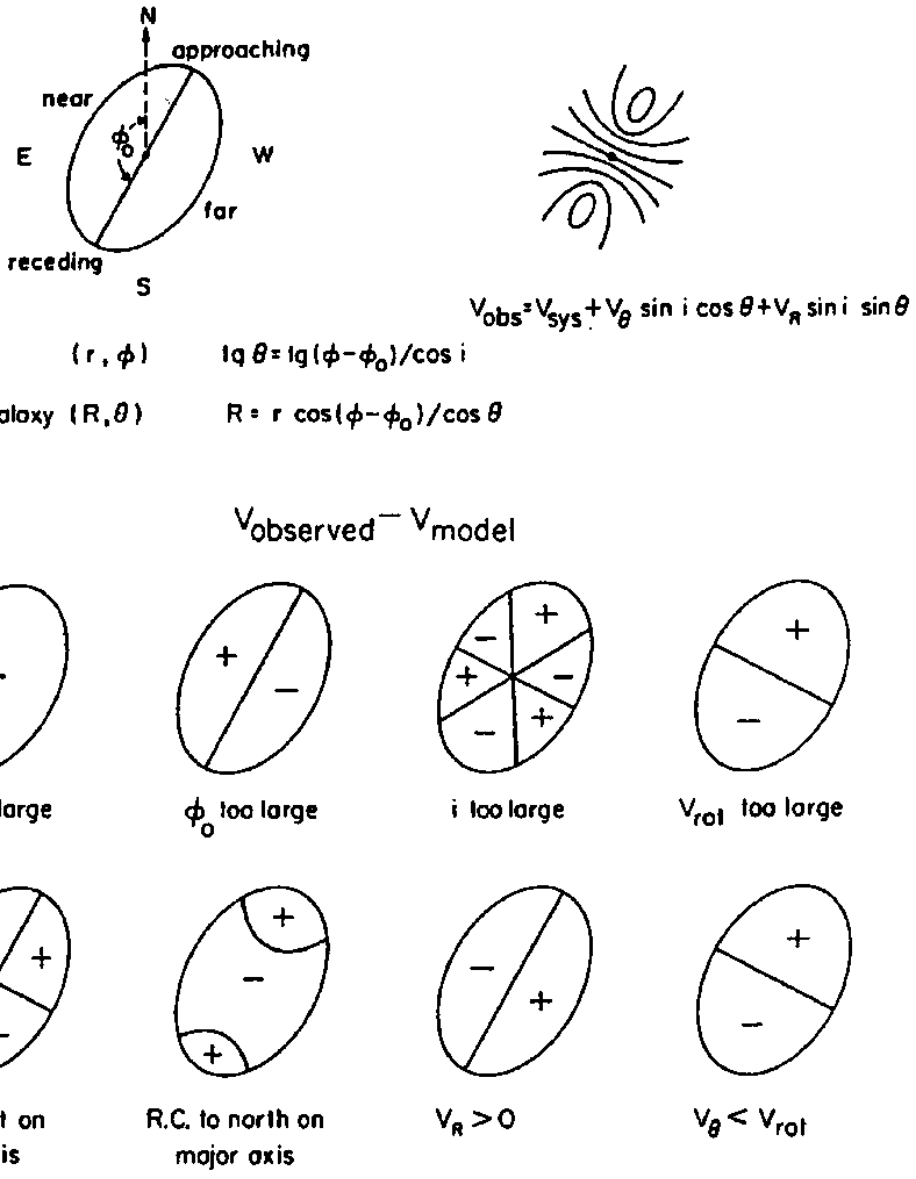

presuppose the profile to have a particular functional form, so that higher order moments can in principle also be calculated. However, these are difficult to measure and Gaussian profiles are usually assumed as soon as one starts to interprete velocity dispersions. The fitting of Gaussians can be done automatically without human interference. The two methods have been compared in detail for the determination of the HI velocity dispersion in face-on spirals from Westerbork maps by van der Kruit and Shostak (1982), using the data on NGC 3938. It turns out that for the window method the personal bias is small

Figure 10.7: Schematic representation of the rotation of disk galaxies and the determination of dynamical parameters. A galaxy with the orientation at top-left shows a pattern of line-of-sight velocities at top-right, where lines of equal radial velocity are sketched. The contours close around the radius of maximum rotation velocity on the line of nodes; a flat rotation curve will fail to show this feature. The relevant equations are then given. The systematic pattern of residual velocities is then shown for the case that all but one of the dynamical parameters are chosen correctly. Note that the patterns are different so that these parameters can be fitted independently to the observed velocity field. The last two examples show the effects of noncircular motion in the radial and tangential direction. From van der Kruit and Allen (1978).

and that for the integrated emission and velocities both methods give very similar results. However, for the determination of velocity dispersions the fitting of Gaussians is to be preferred, but one always has to check how well the observed profiles are actually fitted by Gauss functions. For HI in undisturbed galaxy disks this is in general the case. In area's of low signal-to noise the window method usually produces a superior estimate for the surface densities.

The observed velocity fields across disks of galaxies are almost always dominated by the pattern indicative of circular rotation. From this one then wants to derive a rotation curve $V_{\rm rot}(R)$, which specifies the rotational velocity as a function of galactocentric distance. The usual procedure is to use a least-squares scheme to determine five parameters: position of the rotation center (two numbers), systemic velocity $V_{\rm sys}$, inclination i of the normal to the galaxy plane with the line of sight (so 0° is face-on) and the position angle $\phi_{\rm o}$ of the line of nodes (major axis). These parameters are determined from different symmetry properties of the observed velocity field, as is illustrated in fig. 10.7. Note, however that a systematic pattern of radial expansion or contraction has an effect similar to a change in $\phi_{\rm o}$. Furthermore, deviations in the velocities owing, for example, to a density wave may perturb the derived rotation curve; a detailed self-consistent model has to be used to extract an estimate of the unperturbed rotation curve in that case. Finally, a transverse motion of the galaxy perpendicular to the line of sight produces errors both in $\phi_{\rm o}$ and $V_{\rm rot}(R)$, but these effects are only appreciable for galaxies of large angular size. Lately, various refinements have been used in view of the observation that HI layers often deviate from a single plane beyond the optical extent of the disk, such as determining i and $\phi_{\rm o}$ as a function of galactocentric distance by analyzing the velocity field in annular rings.

These methods of analysis can be applied to all observations of a data-cube as described, radio or Fabry-Perot interferometry. I will illustrate some important results for the case of HI synthesis. First I choose NGC 628 (Shostak and van der Kruit, 1984) to show the derivation of a rotation curve, a warp and the HI velocity dispersion. This is

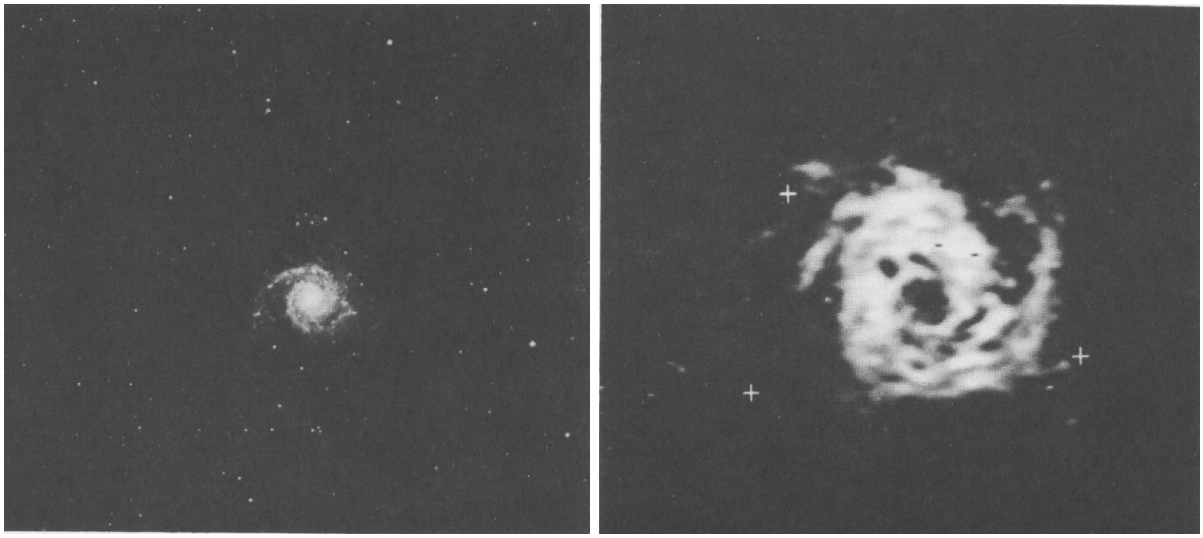

Figure 10.8: Distributions of optical light and HI gas in NGC 628 represented on the same scale. The HI spiral structure in the inner regions fit onto the optical arms, but in the gas these extend out to much larger radii. The two sharp feature in the HI map are processing artifacts and the crosses indicate positions of field stars. From van der Kruit and Shostak (1983).

a rather face-on system, so that the velocity variation due to rotation over a resolution element (telescope beam) is smaller than the effect of velocity dispersion. First we have in fig. 10.8 the integrated HI surface density. The gas is much more extended than the optical disk and, although this is somewhat extreme in NGC 628, this is a general property of disks. A close inspection shows that the HI has maxima on top of the optical spiral arms and these gaseous spiral arms actually continue beyond the extent of the optical structure. Also note the hole of HI in the inner regions, which is a feature common to many spirals.

A general feature of the radial HI distributions is that, at least beyond a central hole, if present, it declines much slower than the optical surface brightness. For Sb and Sc galaxies typical values of this ratio are 10^{-1} $M_\odot/L_{\odot,\mathrm{B}}$ in the inner regions to a few at the optical edges (see e.g. Wevers et al., 1986). In earlier types the general HI surface density is lower, but the amount of variation is similar. The largest HI surface density that occurs in late-type spirals is usually about 8.0 $M_\odot$ pc^{-2}.

The radial distribution of CO and therefore probably also of H_2 has been derived now in a fair number of spirals. A recent review has been given by Young (1987). In Sc galaxies the azimuthally averaged intensities of CO peak in the center and decrease with radius in the disk. The distributions of Hα, optical and radio continuum surface brightness

are similar, which can be interpreted to mean that the massive star forming efficiency is constant with radius, since massive stars appear to form exclusively in molecular clouds. This similarity also means that the ratio of molecular to atomic hydrogen decreases as fast as given above for HI to optical light. In Sa and Sb galaxies at least 40% (improved resolution may increase this number) show a central hole in their CO distributions, similar to that observed in our Galaxy. At present none of the observed Sc galaxies have CO distributions resembling that in the Milky Way.

The observed HI-velocity field of NGC 628 is given in fig. 10.9. At first glance this looks very disturbed, but some general features appear upon closer inspection. First notice that over roughly the optical extent we can discern a pattern as drawn schematically in fig. 10.7 with the dynamical major axis in a position angle of about 30°. This part can be fitted well be the procedure described above, although because of the low inclination the result is in this case insensitive to the value of i. The observed rotation curve has an amplitude of about 25 km s^{-1} in the line of sight. From the integrated luminosity and the Tully-Fisher relation we can estimate the inclination-corrected rotation amplitude and from this an inclination of 5 to 7° can be estimated. We can subtract the symmetric rotation field corresponding to the fit from the observed velocities and obtain a field of residual velocities. This field has an r.m.s. value of only 3.9 km s^{-1} and displays no systematic pattern; this shows that there are essentially no vertical motions in excess of a few km s^{-1}, unless an organized field of such motions exists, such that it mimics in the line of sight that of circular rotation. This is very unlikely and the result therefore indicates an extreme flatness of the disk. For comparison, we can calculate the vertical amplitude of motion, if the HI layer in the solar neighborhood had a z-velocity of 4 km s^{-1}. This is only 45 pc, which illustrates that the HI disk of NGC 628 has to be flat to within values of this magnitude.

Further inspection of fig. 10.9 shows that beyond about 7 arcmin (20 kpc) the pattern remains organized, except that the kinematical major axis rotates to position angle about 100°. Furthermore, at this radius the contour at the systemic velocity of 655 km s^{-1} essentially closes around the galaxy (allow for finite resolution effects). This means that the outer HI layer changes orientation with respect to the inner plane and actually is in the plane of the sky at 20 kpc radius. The angle in space between the outermost ring and the inner plane is small, namely no more than 9° or so. Such warps (except in very special situations) always produce effects of a changing kinematical major axis in the observed velocity field, although the effects on a contour diagram as in fig. 10.9 are usually less pronounced (e.g. see Bosma, 1981a,b).

Next I turn to the velocity dispersions, which are derived by fitting Gaussians to each profile. These fits were always satisfactory and show no evidence for superpositions of two Gaussians ("tails" to the profile). In fig. 10.10 the values have been illustrated by the distribution in the (velocity dispersion, HI surface density) plane. The area of the

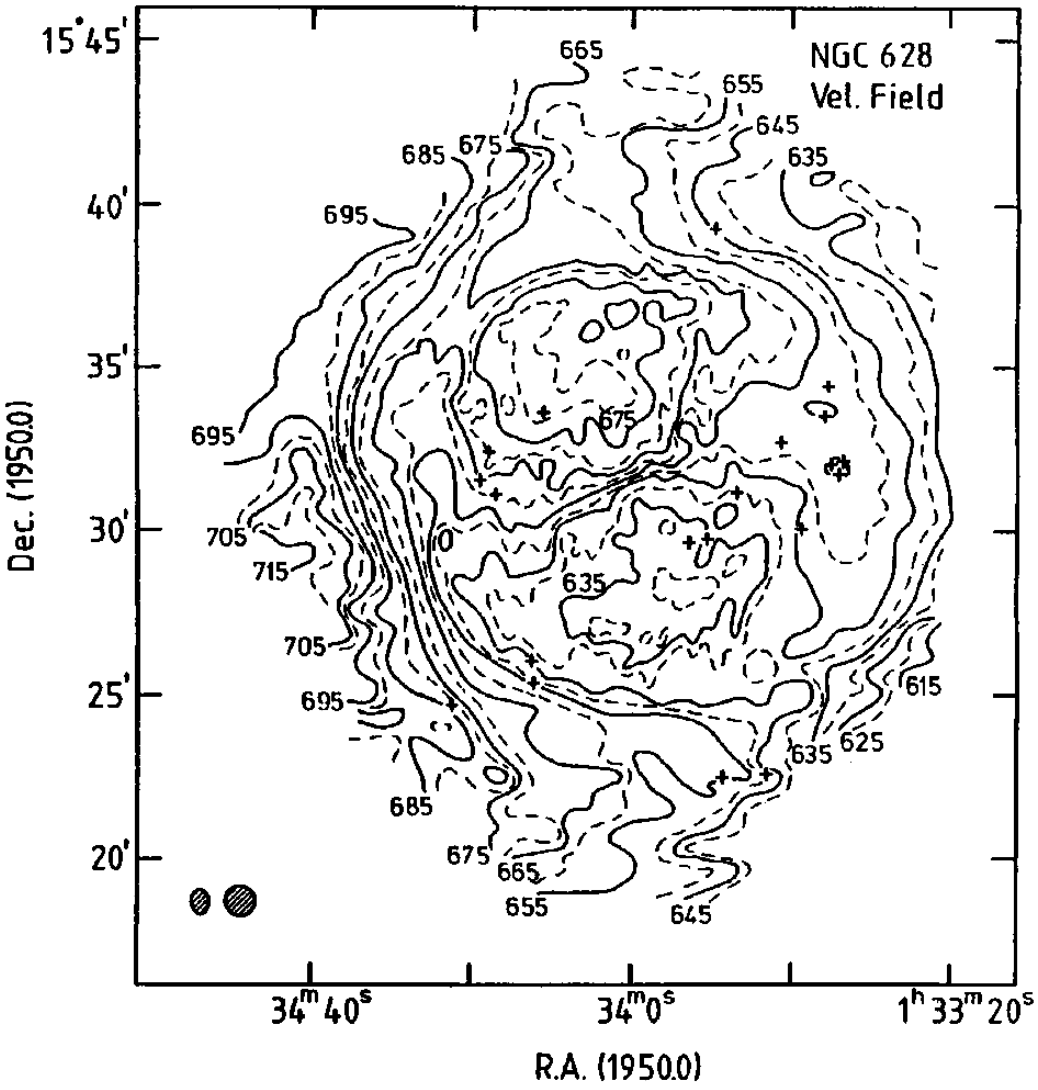

Figure 10.9: The observed radial velocity field of NGC 628. The resolutions used are indicated at the bottom-left and are 1 arcmin FWHM for the outer regions and 14 × 48 arcsec in the inner parts. Contours are shown every 5 km s^{-1}. The velocity field is smooth down to this resolution and continuous contours can be drawn. After Shostak and van der Kruit (1984).

symbol indicates the number of gridpoints at which the values occurred. For this diagram the area between 1.5 and 4.5 arcmin (5 to 15 kpc) has been selected only and regions

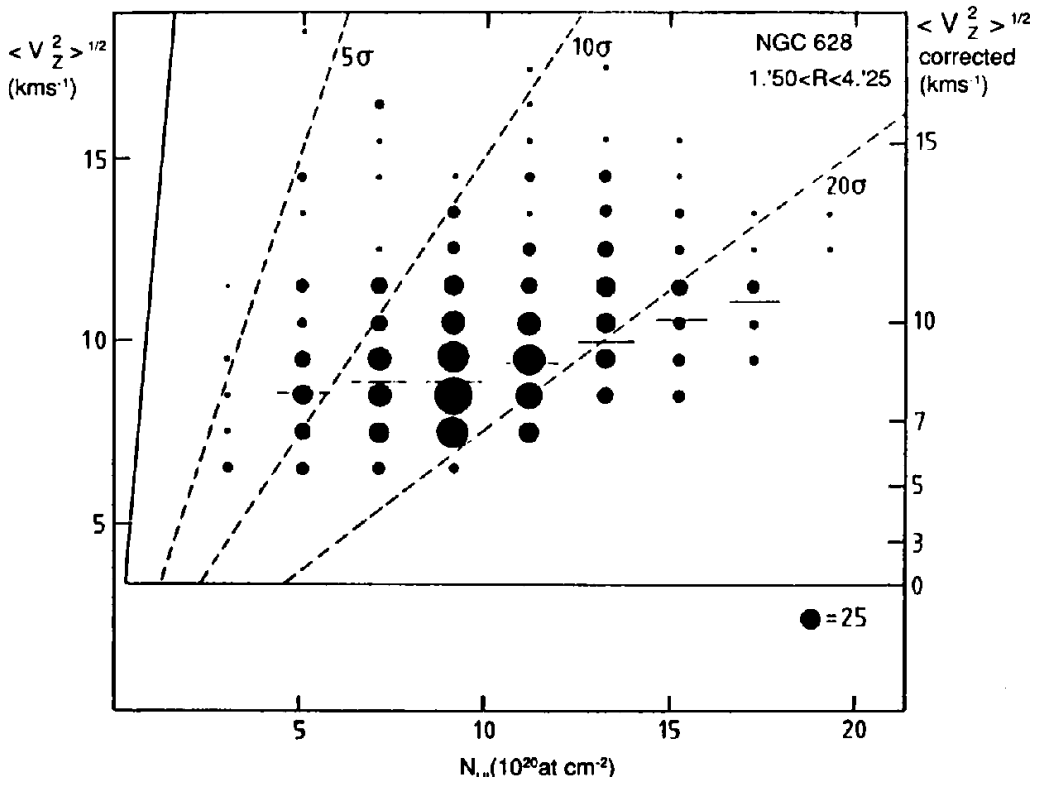

Figure 10.10: The distribution of points over the (HI surface density, velocity dispersion) plane in the inner disk of NGC 628. The area of each symbol is proportional to the number of grid points. The horizontal line is at the instrumental velocity resolution of 3.5 km s^{-1} and at the right are the corrected velocity dispersions. Points to the left of the full-drawn, slanted line have peak surface brightnesses in the profiles less than that where Gaussian fits can be attempted. The dashed lines indicate the peak surface brightnesses of the Gaussians expressed in units of the r.m.s. noise in the channel maps. Profiles in which this is less than 5 are rejected by the automatic routine, because then the formal error in the profile area would exceed 25%. The horizontal bars are the medians of the vertical distributions and appear to increase with surface density. Generally speaking, $n(HI) > 10\ 10^{20}$ H-atoms cm^{-2} correspond to the spiral arms. From Shostak and van der Kruit (1984).

near the minor axis have also been deleted. These area's have been excluded because there the gradient of observed velocity across the telescope beam is too large to derive the velocity dispersion. At each vertical set of points a small horizontal line indicates the median and we see that it increases from about 7 km s^{-1} in low surface brightness regions

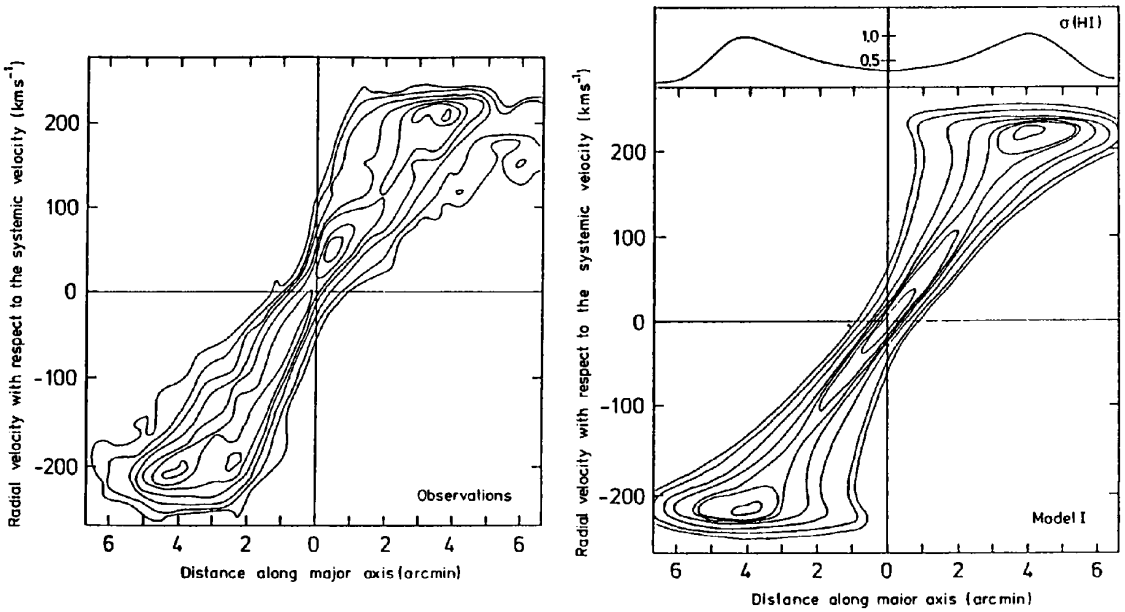

Figure 10.11: (a). The observed HI intensities of NGC 891 in the $l - V$ diagram adapted from Sancisi and Allen (1979), where l is measured along the major axis. Contour levels are in relative units 0.5, 1.0 and in steps of 1.0 up to 6.0. (b) The HI intensities for the model in the same relative units. In this model the derived radial HI distribution is given at the top; the peak value corresponds to 3.7 $M_\odot$ pc^{-2} and the radial distance of this peak is 11 kpc. The derived rotation curve rises from the center to 225 km s^{-1} at 0.25 arcmin (0.7 kpc) and remains constant at this level for larger radii. From van der Kruit (1981).

(the "interarm" regions) to about 10 km s^{-1} in the arms. However, there is no radial dependence of the HI velocity dispersion.

The velocity dispersion of the gas is likely to be isotropic as a result of the frequent collisions of gas clouds. There is no obvious reason, why the HI velocity dispersions always come out about 7 to 10 km s^{-1} in all galaxies observed so far (see van der Kruit and Shostak, 1984). It is however interesting to note that neutral interstellar gas has a very sharp rise in the curve of cooling rate versus temperature at about 10^4 K due to ionization of the hydrogen. For sufficient heat input the gas will thus always get warmer until it reaches this temperature and then will start to cool very efficiently. A kinetic temperature of 10^4 K interestingly corresponds to a one-dimensional velocity dispersion of 9 km s^{-1}. The difference between arm and interarm may simply be the result of heat input from young O and B stars in the spiral arms.

I will now turn to an edge-on galaxy, NGC 891 to illustrate measurements of the thickness of the HI layer as a function of galactocentric distance. The data are from Sancisi and Allen (1979). In such a case we have to deal with line of sight effects and the profiles are certainly not Gaussian as a result of this. The basic data can now be given in an $l - V$ diagram, where l is measured along the galaxy's major axis (see fig. 10.11a). Sancisi and Allen have pointed out how this diagram maps the galactic plane. At a distance r along the major axis the various parts of the line of sight map unto different observed velocities as follows. On the line of nodes we observe the full rotation, but moving away from this line a smaller part of the rotation velocity projects onto the line of sight and therefore the observed velocity approaches more and more the systemic velocity. For example at $l = 3$ arcmin, the line of nodes is seen at about 225 km s^{-1} with respect to systemic, while the edge of the HI along this line of sight occurs at about 70 km s^{-1}. The upper envelope of the HI distribution then corresponds to the rotation curve, except for an amount dependent on the velocity dispersion. This one-to-one mapping of the galaxy's plane onto the diagram is of course similar to the interpretation of the $l - V$ diagrams in traditional HI studies in the Galaxy. The first step in interpreting fig. 10.11 then is to model the observed diagram in a radial distribution of the HI and a rotation curve, using circular symmetry and a value for the HI velocity dispersion. For this purpose one needs to simulate the observational procedure (angular and velocity resolution) in the calculations. The best fitting solution is illustrated in fig. 10.11b.

One can use the data-cube to derive the distribution of the thickness of the HI-layer over the $l - V$ diagram. For this purpose Sancisi and Allen derived the equivalent width, which is at each position in this diagram the sum of HI over all points perpendicular to the major axis, divided by the value in the plane. The result is given in fig. 10.12a. One can see there that the largest equivalent widths are at each l closest to the systemic velocity and therefore at the radial boundaries of the HI distribution. As Sancisi and Allen pointed out qualitatively and as was subsequently confirmed quantitatively, line-of-sight effects will have a significant influence on this diagram in case the inclination deviates slightly from 90°. Fortunately, the signature of inclination and layer-thickening are different across the diagram; the widths at the line of nodes (at each l the maximum deviation from systemic velocity) is not affected by inclination. Detailed modeling, taking again the observational resolutions into account, is necessary for a detailed interpretation.

Let us first see what to expect in an exponential disk with constant M/L. In the isothermal disk with a vertical scale parameter z_o, the vertical distribution of a second component, moving in this force-field with a velocity dispersion $\langle V_z^2 \rangle_g^{1/2}$, will be

$$\rho_g(z, R) = \rho_g(0, R)\mathrm{sech}^{2p}(z/z_o), \text{ where } p = \frac{\langle V_z^2 \rangle_*}{\langle V_z^2 \rangle_g}. \tag{10.16}$$

In disks the velocity dispersion of the gas is considerably smaller than that of the stars,

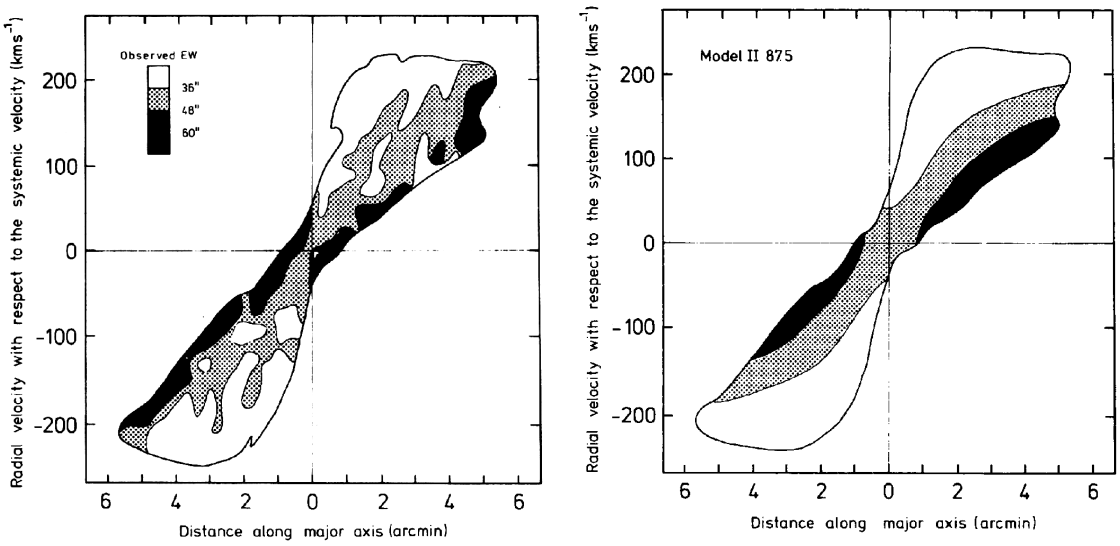

Figure 10.12: (a) The observed equivalent width of the HI layer in the disk of NGC 891 over the $l - V$ diagram, adapted from Sancisi and Allen (1979). (b) The best fitting model for the observed equivalent width, derived from detailed modeling as described in the text. This involves a gradual thickening of the HI layer with galactocentric distance and an inclination of 87°.5. From van der Kruit (1981).

so that p is larger than unity and may possibly approach unity at the edges. Now we can calculate from this the full width of the HI-layer at half-density points (FWHM) as

$$\begin{aligned} \mathrm{FWHM_g} &= 1.6625\, p^{-1/2} z_\mathrm{o} \qquad \text{for} \quad p \gg 1, \\ \mathrm{FWHM_g} &= 1.7628\, z_\mathrm{o} \qquad\quad \text{for} \quad p = 1. \end{aligned} \tag{10.17}$$

With the equation for z_o this becomes then to within 3%

$$\mathrm{FWHM_g} = 1.7 \langle V_\mathrm{z}^2 \rangle_\mathrm{g}^{1/2} \left[\frac{z_0}{\pi G (M/L) \mu_\mathrm{o}} \right]^{1/2} \exp\,(R/2h), \tag{10.18}$$

so that the thickness of the HI layer increases exponentially with an e-folding of two optical scalelengths, if the gas velocity dispersion is constant with radius as observed in face-on systems.

When this thickening of the gas layer is taken, modelling of the diagram in fig. 10.12a results in a best fit, which is illustrated in fig. 10.12b. As described above this procedure involves both a determination of the inclination and of the parameters of the HI thickness.

The fit is good and implies that in NGC 891 $\mathrm{FWHM_g} = (0.22 \pm 0.02)$ exp $(R/2h)$ kpc with $h = 4.9$ kpc and that the inclination is about 87°.5. This can again be taken as evidence that (M/L) of the old disk population is not a function of radius.

The thickening of the HI-layer has also been observed in the Galaxy and possibly in the Andromeda galaxy. It is therefore interesting that Bottema et al. (1986) found that no such thickening is apparent in NGC 5023. It is true that this is a dwarf galaxy with a disk radius of only 7.8 kpc and an extent in HI of about 10 kpc. In this dwarf the HI seems at all radii to have the same thickness as the stellar disk, which also is rather blue with $(U - B)$ about 0.0 and $(B - V)$ about 0.4. A possibility is that star formation here is so vigorous that especially in the inner parts the gas is heated much more efficiently than in larger spirals and that as a result of this the HI does have a variation in velocity dispersion with radius. This is consistent with the HI observations, but cannot be proven from these data.

Finally I will summarize the observations of warps in the HI layers. The presence of such deviations of the gas layer from the inner flat plane was first found in the Galaxy and was inferred from the change in kinematical major axis in M83 by Rogstad et al. (1974) and modeled with the methods involving rings with changing orientations as described above ("tilted ring model"). Another example of such a warp has already been described above for NGC 628. The most direct way to look for warps is of course in edge-on galaxies. Sancisi (1976) has found warps in the HI distribution in four out of five systems and work since then both on edge-on and moderately inclined galaxies has confirmed that warps are the rule rather than the exception (Bosma, 1981a,b). One of these exceptions is NGC 891, the galaxy that has just been described. The largest regular warp has been identified by Bottema et al. (1987) in the edge-on galaxy NGC 4013. There the warp sets in at precisely the edge of the optical disk (9.5 kpc) and reaches a height of about 6 kpc from the inner plane at a distance of 20 kpc from the center. The warp is extremely symmetric between the two sides. The inner disk has a flat rotation curve at 195 km $\mathrm{s^{-1}}$, which suddenly drops to about 170 km $\mathrm{s^{-1}}$ at the edge of the stellar disk and the start of the warp, after which it remains constant up to the last measured point.

10.5 The distribution of mass in spiral galaxies

The distribution of mass in a spiral galaxy can be inferred from the rotation curve. Freeman (1970) has calculated what rotation curve to expect from an exponential disk with constant M/L. The result for an infinitely flat disk is

$$V_{\mathrm{rot}}(R) = (\pi G h \sigma_{\mathrm{o}})^{1/2} \left(\frac{R}{h}\right) \left[I_{\mathrm{o}}\left(\frac{R}{2h}\right) K_{\mathrm{o}}\left(\frac{R}{2h}\right) - I_{1}\left(\frac{R}{2h}\right) K_{1}\left(\frac{R}{2h}\right)\right]^{1/2}. \qquad (10.19)$$

I and K are modified Bessel functions. This curve has a maximum at about 2.2 scalelengths and then declines steadily and eventually Keplerian. The value of the maximum is

$$V_{\rm max} = 0.8796\,(\pi G h \sigma_{\rm o})^{1/2}. \tag{10.20}$$

Allowing for the finite thickness of the disk lowers this value by e.g. 4.5% for the case that $h/z_{\rm o} = 5$.

The discovery of the flat rotation curves in the HI out to large radii (Roberts, 1975; Bosma 1981a,b) has immediately shown that the light distribution alone cannot account for the observed curves if a constant M/L is assumed. Bosma and van der Kruit (1979) observed six spirals in HI and in the optical and inferred what change in M/L would be required if all the mass indicated by the rotation curve were in the disk. This gave local values of M/L order ten (in solar B-units) in the inner regions, after which it increased steadily and reached values of a few hundred at the edges of the optical disks. Since the flat rotation curves continue beyond these edges there must be material with even much higher values there.

It now generally assumed that the material with high M/L is distributed in a more or less spherical "dark halo", of which the constitution remains to be determined. This fits with the evidence for constant M/L in disks and will be discussed in somewhat more detail below. Carignan and Freeman (1985) have proposed to model the rotation curves with a combination of two components, one from the observed distribution of surface brightness (if necessary composed of a disk and a bulge) and an isothermal sphere. They fitted the inner rotation curve to that expected from the light distribution and added then an isothermal sphere to represent the outer part of the rotation curve. This worked satisfactorily in most cases.

Van Albada et al. (1985) have followed a similar scheme, except that they chose a somewhat different form for the density distribution in the dark halo (see below). In fitting the HI observations of NGC 3198 they found that satisfactory fits could be found for a large range of values for the M/L of the disk, all the way from zero (no disk!) to 3.6 in the B-band. The last solution (the "maximum disk" model) gives an amplitude of the rotation curve from the disk alone that is almost equal to that of the outer flat rotation speed and consequently gives rise to a "disk – halo conspiracy". Kent (1986) followed the same procedure and found that features in the rotation curve could be reproduced from features in the light distribution and it was therefore argued that the disk must contribute dominantly to the inner rotation curve and that therefore the solution to be preferred in practice would be the maximum disk model or one very close to this.

Begeman (1987) has made sensitive HI observations of eight spirals in an attempt to trace out rotation curves to as large a distance as possible relative to the optical scalelength h. His record came with NGC 2841, in which HI could be detected out to 17.8 h ($h = 2.4$ kpc in this galaxy, so the HI extends out to 42.6 kpc). The analysis proceeds as follows.

The disk surface density $\sigma(r) = L(r)\ (M/L)$ can for a flat distribution be translated in a circular velocity curve with (Casertano, 1983)

$$V_{\rm c}^2(R) = -8GR \int_0^\infty r \int_0^\infty \frac{\partial \rho(r,z)}{\partial z}\ \frac{K(p) - E(p)}{(Rrp)^{1/2}}\, dz\, dr, \tag{10.21}$$

where $p = x - (x^2-1)^{1/2}$ and $x = (R^2 + r^2 + z^2)/(2Rr)$ and where K and E are complete elliptic integrals. For $\rho(z)$ one may use the isothermal distribution $\mathrm{sech}^2(z/z_{\rm o})$.

The bulge is assumed to be spherical with an observed surface density distribution $\sigma(r) = \mu(r)\ (M/L)$ (where M/L may of course be different from that of the disk) and then (Kent, 1986)

$$V_{\rm c}^2(R) = \frac{2\pi G}{R} \int_0^{\rm R} r\sigma(r)\, dr\ + \frac{4G}{R} \int_{\rm R}^\infty \left[\arcsin\left(\frac{R}{r}\right) - \frac{R}{(r^2 - R^2)^{1/2}} \right] r\sigma(r) dr. \tag{10.22}$$

The halo density distribution is assumed to be

$$\rho(R) = \rho_{\rm o}\ \left[1 + \left(\frac{R}{R_{\rm c}} \right)^2 \right]^{-1}, \tag{10.23}$$

which gives a circular velocity curve

$$V_{\rm c}^2(R) = 4\pi G \rho_{\rm o} R_{\rm c}^2\ \left[1 - \left(\frac{R_{\rm c}}{R} \right) \arctan\left(\frac{R}{R_{\rm c}} \right) \right]. \tag{10.24}$$

This is indeed a flat curve for large R and the asymptotic value is $(4\pi G \rho_{\rm o} R_{\rm c}^2)^{1/2}$.

The contributions from these components have to be added in quadrature to calculate the "total" rotation curve.

The fitting procedure then is as follows. From the observed light distributions the shape of the circular velocity curves of disk and bulge can be calculated, which have to be scaled by a linear factor that depends on the value of M/L. In the same way the contribution of the gas is calculated, but there is no necessity to scale this, since the surface density is measured (25% He is assumed). As a first guess for the disk and bulge M/L the inner rotation curve is represented by the luminous components only (luminous includes the gas). Then the halo is added with a first guess at $R_{\rm c}$ (which determines the shape) and the amplitude is derived by least squares fitting. The M/L's of disk and bulge need to be adapted (decreased) and these are then varied and for each combination a χ^2 is calculated and the best fit is selected. This process is repeated for different values of $R_{\rm c}$ until the final best fit is obtained. Since this process starts out with the largest possible value for M/L of the disk, which then is decreased only to accommodate the dark halo, the final solution has still the largest possible M/L and therefore this is a "maximum disk" fit.

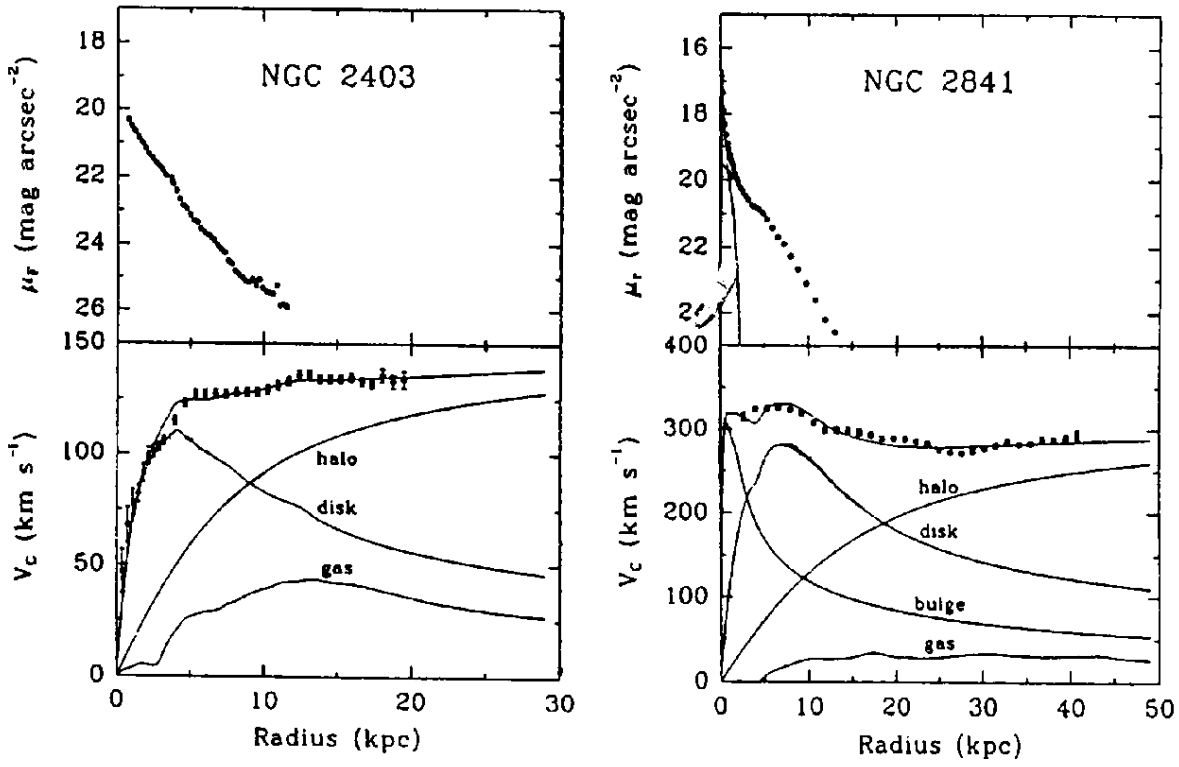

Figure 10.13: Analysis of the rotation curve and mass model for NGC 2403 and 2841. The upper panel shows the photometry from Kent (1987) and a decomposition in truncated bulge and disk. The lower panel shows the observed rotation curve (points and error bars), the circular velocity curves for the four components and the total model rotation curve for the best fitting model. From Begeman (1987).

The result for NGC 2403 and 2841 is shown in fig. 10.13. The photometry in the top panel is from Kent (1987) and is represented by a (truncated) bulge and a disk. The lower panel shows the observations, the four contributing circular velocity curves and the total model rotation curve. Note that the amplitude of the disk circular velocity curve is similar to the asymptotic value for the dark halo. The M/L of the disk is 1.8 for NGC 2403 and for NGC 2841 9.4 and that of the halo 5.6 for NGC 2841. Within the optical boundaries (14 kpc) the mass of the halo constitutes 34% of the total mass and within the outermost point (44 kpc) the dark mass constitutes 79% of the total mass, which is 5.9 10^{11} $M_{\odot}$. For his other seven galaxies Begeman finds M/L's of the disk of 3.1±1.2, so NGC 2841 is here somewhat exceptional. In one case (NGC 5371) there is no need to introduce a dark halo in order to arrive at a fit, but here the rotation curve is observed

out to only 4 scalelengths. For the remaining galaxies the dark mass makes up 44±9% of the total mass within the optical boundaries. For the sample (except NGC 5371) the parameters of the dark halos have ranges of 0.008 to 0.036 $M_\odot$ pc^{-3} for ρ_o and 2.5 to 15 kpc for R_c. The ratio of dark to total matter (Λ) at the largest radius R_M where HI is observed varies between 0.84 and 0.64. The ratio of Λ and R_M (expressed in optical scalelengths h) is 0.072±0.019 and Λ increases with R_M/h, as expected.

It should be stressed that the maximum disk hypothesis implicitly assumed in the modeling above, has some, although not very strong observational support. The support mainly comes from the fact that there are features in some rotation curves that appear to correspond to features in the luminosity profiles. However, the correspondence is not always present and in many cases features in either the rotation curve or the luminosity profile are not accompanied by features in the other. There are also cases where the luminosity profile is affected by spiral structure and where it actually is the contribution from the HI that appears responsible for the structure in the rotation curve. It is therefore of great importance to see whether there is other evidence and this could come from independent ways of measuring the disk mass. Before discussing these I will first look at the values of disk M/L that are implied by the maximum disk hypothesis.

Begeman has, as described above, found that the maximum disk solutions imply values for M/L in the rough range 2 to 5 in solar B-units, except in NGC 2841, where the value is about 9. It is of importance to see first what values are reasonable in view of information available on the solar neighborhood. The integrated surface density, according to the data from Pioneer 10 (van der Kruit, 1986) is $20 \pm 2 L_{\odot,B}$ pc^{-2}. A lower limit to the surface density comes from just adding the contribution from known stars of 24 $M_\odot$ pc^{-2} (Tinsley, 1981) to that from stellar remnants and gas, for which a minimum estimate is about 10 $M_\odot$ pc^{-2}. Then M/L is at least 1.5 in the usual units. The maximum comes from Bahcall's (1984) determination of the surface density from vertical dynamics as 80 $M_\odot$ pc^{-2}, so that M/L is at most 4.5. The solar neighborhood is not in a region of spiral structure and much young stars, so that the upper limit appears to be a strong one. In any case the values seem "reasonable", except for that for the disk of NGC 2841 of 9.4.

One other way of independently estimating the disk mass and checking the maximum disk hypothesis is to use the fact that disks appear to have sharp edges in their light and therefore probably in their mass distributions. If the latter is also true, then one may expect a feature in the rotation curve at this radius R_{max}, which can be used to constrain the disk density distribution. The effects of a sharp edge were calculated by van der Kruit and Searle (1982a) and by Casertano (1983). Inside R_{max} the rotation curve from a truncated disk is flatter than expected from a pure exponential disk due to the absence of outer material, which would have exerted an outward pull. At R_{max} a rather sudden decline in the disk rotation curve sets in and this signature is more pronounced when the ratio R_{max}/h is smaller. Casertano found that the HI observations of NGC 5907 showed

the signature of the disk truncation and derived from this the relative contributions of the disk and halo to the total mass. Within the optical boundaries the dark mass constitutes 60% of the total mass, which is rather higher than the values found by Begeman in his maximum disk models, which average for this ratio at 44%.

A second example where the signature of the disk truncation may be identified in the rotation curve is NGC 4013 (Bottema et al., 1987). This galaxy with its severe HI warp was already described above. At $R_{\rm max}$ the rotation velocity suddenly drops by 25 km s^{-1} from a inner rotation velocity of 195 km s^{-1} and then again remains flat. The interpretation is that the latter is due to the dark halo and that the drop is the truncation feature of the disk. The model that can fit these data has within the optical boundaries this time that the dark halo has only 25% of the total mass, which is even less than what was found by Begeman. So we see that this method is not yet conclusive.

A more direct way is to use "vertical dynamics", which means the use of vertical density distributions and velocity dispersions to infer the gravitational field of the disk. In the disk the gravitation is almost entirely due to the disk itself. Above we have already seen some applications of this in which it was for example inferred that the disk M/L is constant with radius, but until now I have not estimated values for M/L from these data. The method is of course similar to classical estimates of the local surface density of the disk of our Galaxy, as pioneered by Oort (1932). Above the relevant equations have already been given for the isothermal sheet approximation and I will first extend these to different, but plausible distributions at low z and then discuss the outcomes of these studies. These are important to consider, because the actual distribution of stars and mass at low z does have important effects on the numerical results even though the distribution at larger distances from the plane, where we can interprete optical surface photometry, are the same. So, I will first consider alternatives to the isothermal sheet formulae that do share the property that the density distribution tends to an exponential at larger z. This is partly motivated by the fact that Wainscoat (1986) has found some evidence from surface photometry in the near-infrared in one edge-on galaxy, that the z-dependence continues exponentially to low values of z and does not flatten off as expected from the isothermal sech^2 function.

The isothermal sheet description was originally introduced for two reasons. Firstly, it has the property that at large distances from the plane it approximates an exponential, as indicated by existing observations of edge-on galaxies. Secondly, it is known from the kinematics of stars in the solar neighborhood (e.g. Wielen, 1977) that stars that have ages above a few Gyrs all have roughly the same velocity dispersion, so that the mix of stars should at least moderately far from the plane be dominated by a stellar population with essentially a single velocity dispersion. Since this old disk population indeed has most of the disk mass and appears to be self-gravitating, the isothermal sheet immediately suggests itself, at least for light distributions away from the central dust lane. At low

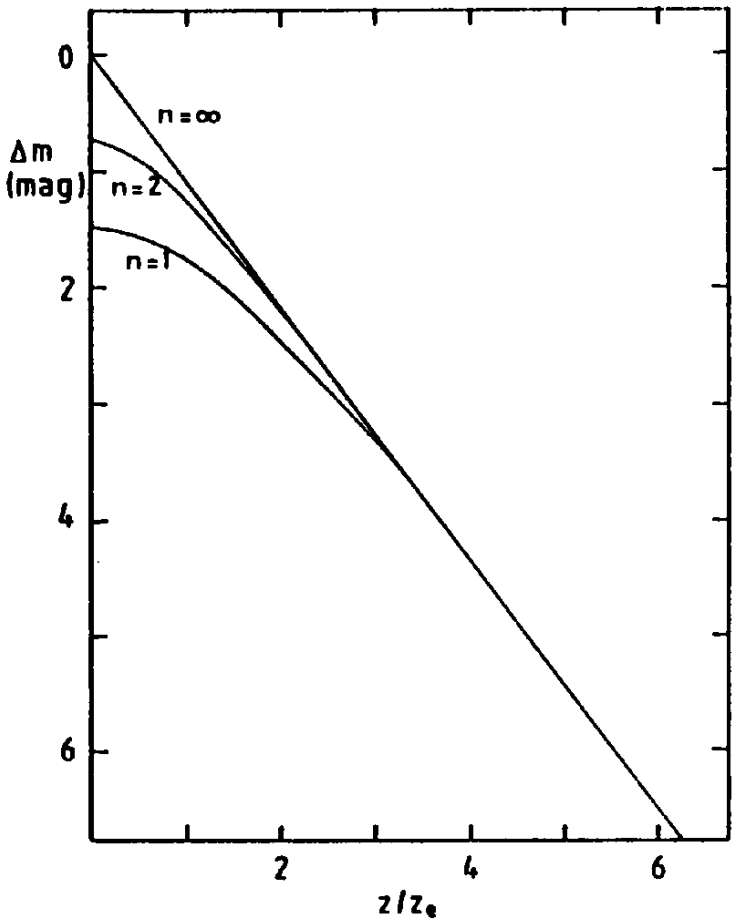

Figure 10.14: The density distribution as a function of distance z from the symmetry plane for the three density models in the text. The parameters have been chosen to give the same density at large z. The vertical scale is in magnitudes. From van der Kruit (1988).

z, however, deviations may be expected, because there the stellar mix may no longer be described as isothermal.

At this point it is not definitely known what distribution for the mass density to use, but it is reasonable to take the sech^2 and an exponential all the way to $z = 0$ as the two extremes. Van der Kruit (1988) has calculated the effects of using the family of density laws

$$\rho(z) = 2^{-2/\mathrm{n}}\rho_{\mathrm{e}}\,\mathrm{sech}^{2/n}(nz/2z_{\mathrm{e}}). \tag{10.25}$$

The isothermal is the extreme for $n = 1$ and the exponential the other for $n = \infty$. Here

ρ_e is the (extrapolated) density in the plane and z_e the exponential scaleheight at large z. For comparison we have for the isothermal sheet $\rho_o = \rho_e/4$ and $z_o = 2z_e$. I will now summarize the relevant equations for both these extreme cases and the intermediate case $n = 2$. The subscripts refer to the value of n. The density distributions are shown in fig. 10.14. The differences are large only at such small z, where in general optical surface photometry cannot be attempted due to dust absorption.

Surface densities:

$$\begin{aligned} \sigma_1 &= \rho_e z_e, \\ \sigma_2 &= (\pi/2)\rho_e z_e, \\ \sigma_\infty &= 2\rho_e z_e. \end{aligned} \tag{10.26}$$

Vertical force K_z, if the distribution is self-gravitating:

$$\begin{aligned} K_{z,1} &= -2\pi G\sigma \tanh(z/2z_e), \\ K_{z,2} &= -4G\sigma \arctan\{\sinh(z/z_e)\}, \\ K_{z,\infty} &= -2\pi G\sigma\{1 - \exp(-z/z_e)\}. \end{aligned} \tag{10.27}$$

Velocity dispersion (squared) at $z = 0$:

$$\begin{aligned} \langle V_z^2\rangle_{o,1} &= 2\pi G\sigma z_e, \\ \langle V_z^2\rangle_{o,2} &= (\pi^2/2)G\sigma z_e, \\ \langle V_z^2\rangle_{o,\infty} &= \pi G\sigma z_e. \end{aligned} \tag{10.28}$$

Velocity dispersion (squared) as a function of z:

$$\begin{aligned} \langle V_z^2\rangle_1 &= \langle W^2\rangle_o, \\ \langle V_z^2\rangle_2 &= \langle W^2\rangle_o\{1 - (2/\pi)^2 \arctan^2(\sinh(z/z_e))\}\cosh(z/z_e), \\ \langle V_z^2\rangle_\infty &= \langle W^2\rangle_o\{2 - \exp(-z/z_e)\}. \end{aligned} \tag{10.29}$$

In a face-on stellar disk the observed velocity dispersion follows from an integration; the values (squared) are

$$\begin{aligned} \langle V_z^2\rangle_{FO,1} &= 2\pi G\sigma z_e, \\ \langle V_z^2\rangle_{FO,2} &= (1.7051)\pi G\sigma z_e, \\ \langle V_z^2\rangle_{FO,\infty} &= (3/2)\pi G\sigma z_e. \end{aligned} \tag{10.30}$$

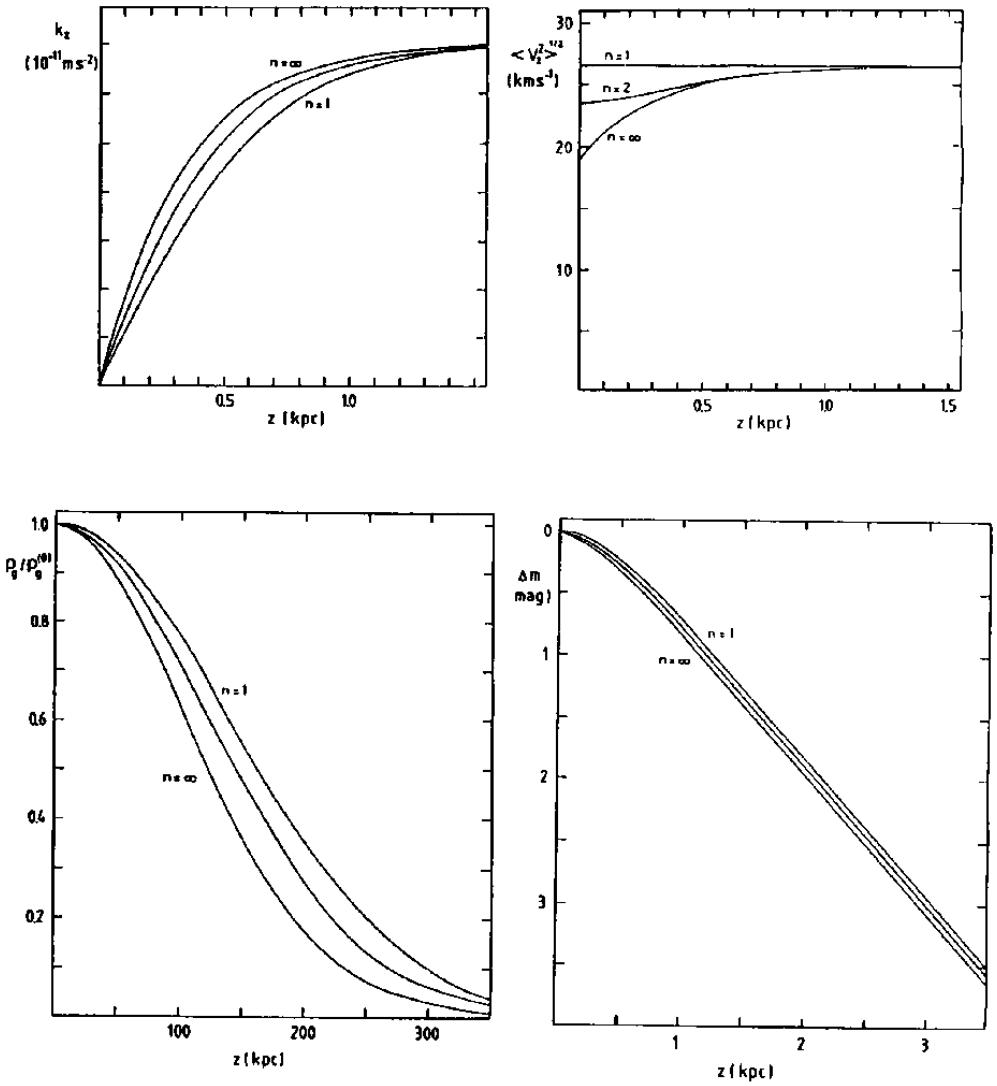

Figure 10.15: Distribution of some properties in the force field of various vertical density distributions, indicated by external galaxies and given in fig. 10.14. All three models have the same integrated surface density of 80 $M_\odot$ pc^{-2} and exponential density slope at large z of 325 pc, typical for the solar neighborhood. (a) The vertical force K_z. (b) The stellar velocity dispersion of the self-gravitating disks. (c) The density distribution of a gas layer with negligible surface density and a velocity dispersion of 8 km s^{-1}. (d) The density distribution of a second isothermal component with negligible surface density and velocity dispersion 45 km s^{-1}. From van der Kruit (1988).

A second non-gravitating component with isothermal velocity dispersion $\langle V_z^2\rangle_{II}^{1/2}$ can be calculated using the parameter

$$p = \frac{\langle V_z^2\rangle_o}{\langle V_z^2\rangle_{II}}. \tag{10.31}$$

The result is

$$\begin{aligned} \rho_{II,1}(z) &= \rho_{II}(0)\mathrm{sech}^{2p}(z/2z_e), \\ \rho_{II,2}(z) &= \rho_{II}(0)\ \exp\ \{-(8/\pi^2)pI(z/z_e)\}, \\ \rho_{II,\infty}(z) &= \rho_{II}(0)\ \exp\ [-2pz/z_e + 2p\{1 -\ \exp\ (-z/z_e)\}]\,. \end{aligned} \tag{10.32}$$

In the second equation the function I follows from

$$I(y) = \int_0^y \arctan(\sinh\, x)\, dx \tag{10.33}$$

An analytical method to calculate this integral and various other useful approximations are given in van der Kruit (1988). In fig. 10.15 are some properties plotted for comparison. In all these cases representative values have been chosen for the solar neighborhood, namely $\sigma = 80\ M_\odot\ \mathrm{pc}^{-2}$ and $z_e = 325$ pc.

We now use these equations to derive values for M/L of the old disk population. First we look at derivations using the observed velocity dispersion of the old disk stars in face-on disks, combined with the observation in edge-on galaxies that $z_e = 0.35 \pm 0.1$ kpc. Van der Kruit and Freeman (1986) have discussed the data in terms of the isothermal sheet approximation only and found for the old disk $M/L = 6 \pm 2$ (as always below in solar B-units). The effects of the two additional models are that it will have to be increased by 17% for $n = 1$ and by 33 % for the exponential model. On this basis we may take as the best determination $M/L = 7.5 \pm 2.5$ after allowance for the uncertainty of which model to choose.

As fig. 10.15c shows, the HI layer is severely affected by the choice of n, understandably because of the fact that the gas resides at small z and is therefore sensitive to the precise form of K_z near the plane. The width of the HI layer at half-density points $\mathrm{FWHM_g}$ can be conveniently be expressed in terms of a length parameter z_g, which equals

$$d_g = \left(\frac{\langle V_z^2\rangle_g z_e}{G\sigma}\right)^{1/2}. \tag{10.34}$$

Then for the three models we have for $p \gg 1$

$$\begin{aligned} \mathrm{FWHM}_{\mathrm{g},1} &= 1.33\, d_{\mathrm{g}}, \\ \mathrm{FWHM}_{\mathrm{g},2} &= 1.18\, d_{\mathrm{g}}, \\ \mathrm{FWHM}_{\mathrm{g},\infty} &= 0.94 d_{\mathrm{g}}. \end{aligned} \tag{10.35}$$

For p of order unity the numerical values need to be decreased by about 7%.

The effects of the different models are rather large, especially when we remember that σ follows from d_{g} squared. The effect on M/L is even more severe, because in edge-on galaxies the face-on surface brightness is determined from fitting to the z-profiles at large z and the isothermal value is a factor two lower than if an exponential were assumed. For the fit to the HI layer in NGC 891 (van der Kruit, 1981) the isothermal approximation gave for the old disk 8±4 and this becomes 4±2 for $n = 2$ and 2±1 for the exponential. So, such HI measurements are only useful to monitor a change in M/L and are not very accurate in determining its value.

The conclusion from such work is that the best value for M/L of the old disk population is 6±2. This cannot yet be compared directly to Begeman's values, because we have to add in the young population. The disk colors can be used for this as a guide. For example in the Bahcall and Soniera (1984) model for the Galaxy, the integrated color of the contributions to the disk surface brightness are $(B-V)$ about 0.56 for old dwarfs, 1.30 for disk giants and −0.03 for young population I (see van der Kruit, 1986). The old disk can on this basis be expected to have a $(B-V)$ of about 0.9 and from the observed colors we may then estimate in a galaxy disk the relative contributions of old disk and young population I. From this it follows that for a typical Sb disk with a $(B-V)$ of 0.65 the M/L would be 4, if for the old disk population only it is 6. For an Sc disk with $(B-V) = 0.4$, the M/L becomes 2. So we can see that these estimates of disk masses result in M/L's in the range 1 to 5 for disks of Sb galaxies or later types and fits with the maximum value of 4.5 quoted above for the Galactic disk. This shows that Begeman's values of 3±1 (excluding NGC 2841) are indeed "reasonable" in view of this. On the other hand the uncertainties are large, so that this must not be taken as a strong confirmation of the maximum disk hypothesis. At this point it therefore is not entirely clear yet that a disk-halo conspiracy indeed exists. This conspiracy expresses the fact that in maximum disk fits the disk-alone and (dark) halo-alone rotation curves have essentially the same amplitude. It is not even clear from the present observations whether the ratio of luminous to dark matter is closely the same in all galaxies.

Now that we have at least some indications of the M/L to be expected in a disk, it is of interest to return to the stability questions raised above. For the local stability I have already indicated that these results lead to values for Toomre's Q in the range of

1.5 to 2 and disks appear stable locally. For global stability Efstathiou et al. (1982) have derived from numerical experiments an empirical parameter Y, which should exceed 1.1 for stability

$$Y = V_{\rm m} \left(\frac{h}{GM_{\rm d}} \right)^{1/2}, \tag{10.36}$$

where $M_{\rm d}$ is the disk mass and $V_{\rm m}$ the velocity in the flat part of the rotation curve. Estimates of this parameter for samples of galaxies with rotation curves and surface photometry give mean values somewhat below the critical value, but it is generally within the uncertainties. On the other hand, I have already indicated above that the observed central velocity dispersions in the disks are sufficiently high to contribute also to global stability. A rough calculation (van der Kruit and Freeman, 1984) shows that the condition $Y = 1.1$ means that within the optical boundaries the dark halo must make up about 75% of the mass. In Begeman's sample this condition is not met, since for his galaxies the maximum disk fits gave values of about 45±10%. So it follows that the maximum disk hypothesis in general implies that $Y < 1.1$ and that therefore the dark halo would not be sufficiently massive in the inner regions to provide global disk stability.

For NGC 891 the value for Y can be calculated more accurately than above, because M/L is not needed here. For the observed thickness of the HI layer van der Kruit (1981) found $\mathrm{FWHM_g} = 0.22 \exp(R/2h)$ kpc and using $z_{\rm e} = 0.49$ kpc the disk central surface density becomes for the three models 266 (isothermal), 210 and 133 (exponential) $M_\odot$ pc^{-2}. With $h = 4.9$ kpc the disk mass becomes respectively 4.0, 3.2 and 2.0 10^{10} $M_\odot$ and the maximum in the "disk-alone" rotation curve 111, 99 and 79 km s^{-1}. This is significantly lower than the observed rotation of 225±10 km s^{-1}. The total mass within $R_{\rm max} = 21$ kpc is about 2 10^{11} $M_\odot$, so the disk does make up only a small fraction of the mass within the optical boundaries. The parameter Y also follows immediately as respectively 1.20, 1.34 and 1.70. So, NGC 891 does not conform to the maximum disk hypothesis (and this is independent of any assumed value for M/L) and the dark halo in this case is massive enough to stabilize the disk against global modes.

There is a interesting coincidence that I want to point out finally in respect to dark halos and the maximum disk hypothesis. Earlier in this course I showed component separations in the light distributions of the two edge-on galaxies NGC 891 and NGC 7814. These are two extremes in the sense that in NGC 891 82% of the light from old stars is in an exponential disk, while for NGC 7814 93% is in an $R^{1/4}$-bulge. In spite of these major differences in the light and therefore the luminous mass distributions, the rotation curves of the two galaxies are very similar, both rising to about 225 km s^{-1} in about 3 kpc and remaining flat thereafter out to at least 20 kpc. This seems to imply that the force field cannot be dominated by the gravitation of the luminous material and must be set by a dark component.

Finally, I note that optical and near-infrared searches have been made for material that

could constitute the dark halos. This has been reviewed recently by van der Kruit (1987) and the conclusion is that H-burning main sequence stars can be ruled out, especially by the measurements in the near-infrared. The local M/L (in B) in the halo is in excess of 1100. IRAS data have not been able to rule out black (or brown) dwarfs, so low mass objects that are below the H-burning limit are still possible.

10.6 The mass distribution in our Galaxy

To conclude this set of lectures I will make a brief comparison to our Galaxy. In the first place I note that the Galaxy's disk velocity dispersion was included in fig. 10.6 above and that it appears to fit in with the trend noted there. In view of the discussion in the previous section it is of interest to see whether or not according to the available data the Galaxy has a "maximum disk". Observations of the rotation curve and the local disk surface density are presented and discussed elsewhere in this course and I will not repeat this. As in essentially all other galaxies, the rotation curve is probably flat and the amplitude will be taken in what follows as 230±15 km s^{-1}. The disk local surface density is currently in some dispute, as discussed in this course by Gilmore, and is either 80±20 $M_\odot$ pc^{-2} following Bahcall (1984) or 45±9 $M_\odot$ pc^{-2} in the Kuyken and Gilmore (1988) analysis. These two determinations are from completely different samples; Bahcall (B84) uses G- and F-dwarfs and K-giants, while Kuyken and Gilmore (KG) base their analysis on their own sample of K-dwarfs.

First let us look at some local properties, that have been discussed above for external galaxies. The first is M/L. The local disk surface brightness was estimated from the Pioneer 10 data in van der Kruit (1986) as 23.8±0.1 B-mag arcsec^{-2} (= 20±2 $L_\odot$ pc^{-2}), so that the total disk M/L becomes respectively 4.0±1.0 (B84) or 2.3±0.5 (KG). It was estimated that the old disk population contributes two-thirds of the surface brightness, so that the old disk M/L can estimated as respectively 6.0±1.5 and 3.5±0.8. The first value is comparable to what was found in external galaxies. Another quantity that can be calculated is Toomre's Q, which for a radial stellar velocity dispersion of 45±5 km s^{-1} comes out as 1.5±0.5 (B84) or 2.7±0.9 (KG). Again the value based on Bahcall's surface density is comparable to that estimated for external disks.

Schmidt (1985) has recently presented a mass model of the Galaxy consisting of three components: a "bulge + spheroid" (which in the nomenclature of this course would simply be called bulge), an exponential disk with a scalelength of 3.5 kpc and a "corona" or dark halo. A revised version of this has been presented in van der Kruit (1986) for a disk scalelength of 5 kpc and has been reproduced in fig. 10.16. The bulge has been left unaltered and constitutes a mass of about 10^{10} $M_\odot$. In this model the local disk surface density has been taken as 80 $M_\odot$ pc^{-2} and its total mass then is 7 10^{10} $M_\odot$. The dark

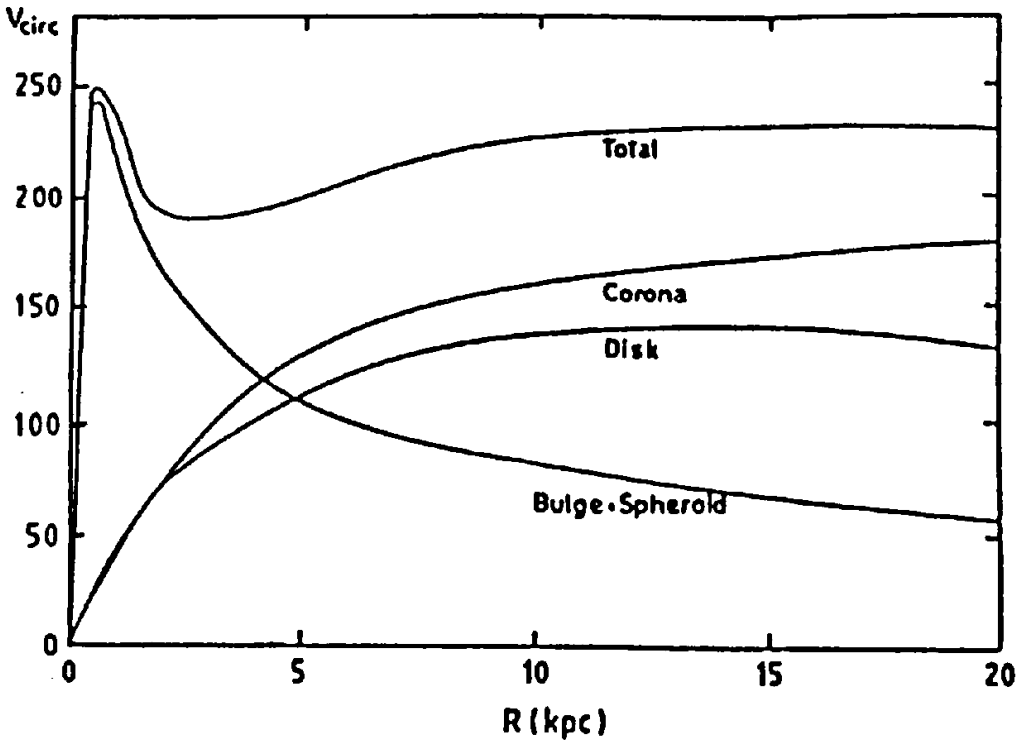

Figure 10.16: Mass model of the Galaxy represented by the rotation curves corresponding to the gravitational fields of the individual components indicated. This is an adaption of the model given by Schmidt (1985), allowing for a disk scalelength of 5 kpc. The sun is at 8.5 kpc from the center. Further parameters of the model are in the text. From van der Kruit (1986).

halo, which Schmidt modeled as $\rho \propto (a^2 + R^2)^{-1}$ has been adapted to $a = 2.8$ kpc and has a mass within the probable disk radius $R_{\rm max} = 25$ kpc of 1.9 10^{11} $M_\odot$. The local mass density in the dark halo is 0.009 $M_\odot$ pc^{-3}. The halo constitutes 70% of the mass within the optical disk radius, which is significantly higher than Begeman's mean value of 45%, which follows from his maximum disk fits. The inferred value for the global stability parameter Y is 0.98±0.25.

The model given has a less massive disk than in the maximum disk hypothesis. Clearly, the local surface density from Kuyken and Gilmore would fail by an even larger margin to accomplish this. We must still see whether the uncertainties actually rule out a maximum disk model for the Galaxy. From the maximum disk fits in other galaxies, such a model would imply that the disk-alone rotation curve would need to have an amplitude of 195 km s^{-1} or more. The disk in the model in fig. 10.16 has a maximum rotation of about 135

km s^{-1}. To have an amplitude of 195 km s^{-1} the disk would need to have a local surface density of about 140 $M_\odot$ pc^{-2}, if the disk scalelength is 5 kpc, but this can be brought down to 100 $M_\odot$ pc^{-2}, if the scalelength were 3.5 kpc. This in itself would imply that our Galaxy is probably not maximum disk, but we should really interprete maximum disk to mean that all the luminous material (disk and bulge) by itself should be able to explain the amplitude (or most of it) of the inner rotation curve. From fig. 10.16 we see that at the solar position the bulge- alone rotation curve has an amplitude of about 80 km s^{-1} and therefore the amplitude of the rotation curve from all the luminous material is in the model about 160 km s^{-1}. This still falls short of the required amplitude in the maximum disk hypothesis.

Sellwood and Sanders (1988) have tried to construct a maximum disk model for the Galaxy by pushing all constraints to their limits. They can accomplish that by assuming a disk scalelength of 4 kpc and a much more massive bulge of (3–4) 10^{10} $M_\odot$ (about 3 or 4 times more than in the model of fig. 10.16). It is especially this bulge mass that allows their solution, but the problem is that the local bulge density then is (4.6–6.3) 10^{-4} $M_\odot$ pc^{-3}, which is at least a factor 2 higher than the best observational constraints (Schmidt, 1985). This bulge mass is also inconsistent with the observed drop in the Galactic rotation curve between 1 and 4 kpc, although it can be argued that this feature is due to absence of gas or non-circular motions in this region. My conclusion still is that our Galaxy is probably not maximum disk. Sellwood and Sanders also note that the Kuyken and Gilmore local surface density would make the solution even more extreme, requiring a local circular velocity of 200 km s^{-1} and a solar galactocentric distance of 9.5 kpc.

10.7 References

Argyle, E. 1965, Astrophys. J. **141**, 750
Athanassoula, E., Sellwood, J.A. 1986, Monthly Notices Roy. Astron. Soc. **221**, 213
Babcock, H.W. 1939, Lick Obs. Bull. **19**, 41
Bahcall, J.N. 1984, Astrophys. J. **287**, 926
Bahcall, J.N., Soniera, R.M. 1984, Astrophys. J. Suppl. **55**, 67
Begeman, K. 1987, Ph.D. Thesis, Univ. of Groningen
Bosma, A. 1981a, Astron. J. **86**, 1791
Bosma, A. 1981b, Astron. J. **86**, 1825
Bosma, A., van der Kruit, P.C. 1979, Astron. Astrophys. **79**, 281
Bottema, R. 1988, Astron. Astrophys. **197**, 105
Bottema, R., Shostak, G.S., van der Kruit, P.C. 1986, Astron. Astrophys. **167**, 34
Bottema, R., Shostak, G.S., van der Kruit, P.C. 1987, Nature **328**, 401
Carignan, C., Freeman, K.C. 1985, Astrophys. J. **294**, 494

Casertano, S. 1983, Monthly Notices Roy. Astron. Soc. **203**, 735
Efstathiou, G., Lake, G., Negroponte, J. 1982, Monthly Notices Roy. Astron. Soc. **199**, 1069
Freeman, K.C. 1970, Astrophys. J. **160**, 811
Goldreich, P., Lynden-Bell, D. 1965, Monthly Notices Roy. Astron. Soc. **130**, 125
Hulst, H.C. van de, Raimond. E., Woerden, H. van 1957, Bull. Astron. Inst. Neth. **14**, 1
Illingworth, G., Freeman, K.C. 1974, Astrophys. J. **188**, L83
Kent, S. 1986, Astron. J. **91**, 1301
Kent, S. 1987, Astron. J. **93**, 816
Kormendy, J., Illingworth, G. 1982, Astrophys. J. **256**, 460
Kormendy, J., Illingworth, G. 1983, Astrophys. J. **265**, 632
Kuyken, K., Gilmore, G. 1988, preprint
Lacey, C.G. 1984, Monthly Notices Roy. Astron. Soc. **208**, 687
Lewis, J.R. 1986, Ph.D. Thesis, Australian Natl. Univ.
Lewis, J.R., Freeman, K.C. 1989, Astron. J. **97**, 139
Martinet, L. 1988, Astron. Astrophys. **206**, 253
Oort, J.H. 1932, Bull. Astron. Inst. Netherlands **6**, 249
Ostriker, J.P., Peebles, P.J.E. 1973, Astrophys. J. **186**, 467
Pease, F.G. 1915, Publ. Astron. Soc. Pacific **27**, 239
Pease, F.G. 1916, Proc. Natl. Acad. Sci. (U.S.) **2**, 517
Pease, F.G. 1918, Proc. Natl. Acad. Sci. (U.S.) **4**, 21
Roberts, M.S. 1975, IAU Symp. **69**, Dynamics of Stellar Systems, ed. A. Hayli, Dordrecht: Reidel, p. 331
Rogstad, D.H., Lockhart, I.A., Wright, M.C.H., 1974, Astrophys. J. **193**, 309
Sancisi, R. 1976, Astron. Astrophys. **53**, 159
Sancisi, R., Allen, R.J. 1979, Astron. Astrophys. **74**, 73
Sargent, W.L.W., Schechter, P.L., Boksenberg, A., Shortridge, K. 1977, Astrophys. J. **212**, 326
Schmidt, M. 1985, IAU Symp. **106**, The Milky Way Galaxy, ed. H. van Woerden, W.B. Burton and R.J. Allen, Dordrecht: Reidel, p. 75
Sellwood, J.A. 1983, IAU Symp. **100**, Internal Kinematics and Dynamics of Galaxies, ed. E. Athanassoula, Dordrecht: Reidel, p. 197
Sellwood, J.A., Carlberg, R.G. 1984, Astrophys. J. **282**, 61
Sellwood, J.A., Sanders, R.H. 1988, Monthly Notices Roy. Astron. Soc. **233**, 611
Shostak, G.S., van der Kruit, P.C. 1984, Astron. Astrophys. **132**, 20
Simkin, S.M. 1971, Astron. Astrophys. **31**, 129
Slipher, V.M. 1914, Lowell Obs. Bull. **II**, No. 12
Spitzer, L., Schwarzschild, M. 1951, Astrophys. J. **114**, 385

Tinsley, B.M. 1981, Astrophys. J. **250**, 758
Tonry, J., Davis, M. 1979, Astron. J. **84**, 1511
Toomre, A. 1964, Astrophys. J. **139**, 1217
van Albada, T.S., Bahcall, J.N., Begeman, K., Sancisi, R. 1985, Astrophys. J. **295**, 305
van der Kruit, P.C. 1981, Astron. Astrophys. **99**, 298
van der Kruit, P.C. 1987, IAU Symp. **117**, Dark Matter in the Universe, ed.: J. Kormendy and G.R. Knapp, Dordrecht: Reidel, p. 415
van der Kruit, P.C. 1986, Astron. Astrophys. **157**, 230
van der Kruit, P.C. 1988, Astron. Astrophys. **192**, 117
van der Kruit, P.C., Allen, R.J. 1978, Ann. Rev. Astron. Astrophys. **16**, 103
van der Kruit, P.C., Freeman, K.C. 1986, Astrophys. J. **303**, 556
van der Kruit, P.C., Searle, L. 1982a, Astron. Astrophys. **110**, 61
van der Kruit, P.C., Searle, L. 1982b, Astron. Astrophys. **110**, 79
van der Kruit, P.C., Shostak, G.S. 1982, Astron. Astrophys. **105**, 351
van der Kruit, P.C., Shostak, G.S. 1984, Astron. Astrophys. **134**, 258
Wainscoat, R.J. 1986, Ph.D. Thesis, Australian Natl. Univ.
Wevers, B.M.H.R., van der Kruit, P.C., Allen, R.J. 1986, Astron. Astrophys. Suppl. **66**, 505
Wielen, R. 1977, Astron. Astrophys. **60**, 263
Wolf. M. 1914, Vierteljahresschrift Astron. Gesell. **49**, 162
Woolley, R.v.d.R. 1978, Monthly Notices Roy. Astron. Soc. **184**, 311
Young, J.S. 1987, Star Formation in Galaxies, NASA Conf. Proc. **2466**, p. 197